NSWC TR 88-166

AD-A219 434

THE COUPLED-MODE METHOD FOR TRANSMISSION LOSS CALCULATION IN A RANGE-DEPENDENT OCEANIC ENVIRONMENT

BY JUAN I. ARVELO, JR.

UNDERWATER SYSTEMS DEPARTMENT

27 FEBRUARY 1989

NAVAL SURFACE WARFARE CENTER

Dahlgren, Virginia 22448-5000 • Silver Spring, Maryland 20903-5000

UNCLASSIFIED

SECURITY CLASSIFICATION OF THIS PAGE

REPORT DOCUMENTATION PAGE

1a. REPORT SECURITY CLASSIFICATION UNCLASSIFIED	1b. RESTRICTIVE MARKINGS
2a. SECURITY CLASSIFICATION AUTHORITY	3. DISTRIBUTION/AVAILABILITY OF REPORT Approved for public release; distribution is unlimited.
2b. DECLASSIFICATION/DOWNGRADING SCHEDULE	
4. PERFORMING ORGANIZATION REPORT NUMBER(S) NSWC TR 88-166	5. MONITORING ORGANIZATION REPORT NUMBER(S)
6a. NAME OF PERFORMING ORGANIZATION Naval Surface Warfare Center 6b. OFFICE SYMBOL (If applicable) U25	7a. NAME OF MONITORING ORGANIZATION
6c. ADDRESS (City, State, and ZIP Code) 10901 New Hampshire Ave. Silver Spring, MD 20903-5000	7b. ADDRESS (City, State, and ZIP Code)
8a. NAME OF FUNDING/SPONSORING ORGANIZATION 8b. OFFICE SYMBOL (If applicable)	9. PROCUREMENT INSTRUMENT IDENTIFICATION NUMBER
8c. ADDRESS (City, State, and ZIP Code)	10. SOURCE OF FUNDING NOS. PROGRAM ELEMENT NO. 61152N; PROJECT NO. R00N0; TASK NO. 11; WORK UNIT NO.

11. TITLE (Include Security Classification) The Coupled-Mode Method for Transmission Loss Calculation in a Range-Dependent Oceanic Environment

12. PERSONAL AUTHOR(S)
Arvelo, Juan I., Jr.

13a. TYPE OF REPORT	13b. TIME COVERED	14. DATE OF REPORT (Yr., Mo., Day)	15. PAGE COUNT
Technical Review	FROM TO	1989, February, 27	104

16. SUPPLEMENTARY NOTATION

17. COSATI CODES			18. SUBJECT TERMS (Continue on reverse if necessary and identify by block number)
FIELD	GROUP	SUB. GR.	Normal Mode, Range-Dependent, Propagation Loss, Mode Coupling, Low-Frequency
20	01		

19. ABSTRACT (Continue on reverse if necessary and identify by block number)

This report presents the coupled normal mode model to calculate the propagation loss of low-frequency acoustic signals in a range-dependent shallow ocean. It also derives the equations to include the effects of the continuous spectrum and the environmental attentuation using the first and second order perturbation terms to the solution of the real eigenequation. The bottom is assumed to have no shear effects and an axially symmetric cylindrical coordinate system is used. Therefore, no bearing dependence of the environment is also assumed in this model. It has been found that the first order perturbation term is purely imaginary, providing the imagery part of the eigenvalues and eigenfunctions. The second order perturbation term is found to be purely real, and it represents a correction to the unperturbed eigenvalues and eigenfunctions. The range-dependent environment is divided into a suitable number of range-independent segments, and the respective modes are calculated in order to couple them to account for the interchange of energy and (Cont.)

20. DISTRIBUTION/AVAILABILITY OF ABSTRACT	21. ABSTRACT SECURITY CLASSIFICATION
X UNCLASSIFIED/UNLIMITED ___ SAME AS RPT ___ DTIC USERS	UNCLASSIFIED

22a. NAME OF RESPONSIBLE INDIVIDUAL	22b. TELEPHONE NUMBER (Include Area Code)	22c. OFFICE SYMBOL
Juan I. Arvelo, Jr.	(202) 394-3428	U25

DD FORM 1473, 84 MAR 83 APR edition may be used until exhausted
All other editions are obsolete

UNCLASSIFIED
SECURITY CLASSIFICATION OF THIS PAGE

19. heat to adjacent modes. A simple environment is used to display the importance of mode coupling in a range-dependent ocean environment.

FOREWORD

This report describes the coupled normal mode model to account for the range-dependence of a shallow ocean environment and for sources of low frequency sound. The effects of absorption have also been added by the method of perturbation. This model can also simulate the transmission loss in deeper environments at the expense of longer computer time (CPU). The author extends his special thanks to Mr. Scott Hebbert for the informal but instructive consultations on computational techniques and for providing some of his plotting routines. Also the encouragement of Mr. John Sherman is greatly appreciated. This work was funded by the Independent Research Board of the Naval Surface Warfare Center.

Approved by:

C. A. KALIVRETENOS, Head
Sensors and Electronics Division

CONTENTS

ILLUSTRATIONS

ILLUSTRATIONS (Cont.)

CHAPTER 1

INTRODUCTION

The normal-mode theory gives the exact solution to the problem of sound propagation in a range-independent oceanic wave-guide. It is well known, however, that the ocean has some range dependence due to changes in the depth of the bottom or changes in the acoustic properties of the environment as shown in Figure 1. From all the acoustic properties, the sound speed is the most range-variable one due to the changes in temperature and pressure. Therefore, a reliable range-dependent method must be created. This range-dependent method must allow for the effects of bottom interaction, including shear wave from the solid sediments and the attenuation coefficient of the compressional and shear wave. The most suitable method for this purpose is the coupled normal-mode method. This method consists in dividing the range-dependent environment into range-independent segments, solve for the eigenvalues and eigenfunctions of these segments using the normal-mode theory, and couple these modes using the coupled range equation and the radial boundary conditions.

The coupled normal-mode method was implicitly originated by Allan Pierce in the late 60's as an adiabatic-mode theory, with eigenray calculations to estimate the coupling coefficients, to simplify the solution to the propagation in a range-dependent environment.[1-4] In this adiabatic mode theory, he assumes isovelocity media and a weak coupling between the natural modes of the wedge-like wave guide. He found that compressional waves

refract into the basement until they get completely attenuated, and his results agreed well with the results from the Parabolic Equation method. McDaniel used the coupled eigen-equations to calculate the energy transferred between normal modes as a result from bottom scattering of the ocean, and has shown that randomly rough sea bed layering can increase the transmission loss depending upon the degree of penetration of the acoustic field into the sediment.[5-8] Evans modeled the axisymmetric range-dependent medium as N range-independent segments with a pressure-release false bottom suitably deep to discretize the continuous spectrum, and isodensity-isovelocity layers to simplify the solutions of the linear wave equation in each layer.[9-11] In this stepwise coupled-mode method he solves for the eigenvalues and eigenfunctions of each range-independent segment by taking into account the absorption of the basement to avoid the reflected energy from the pressure-release false bottom. Überall's group has used a similar method for solving the set of coupled range equations, but assuming layers of linear index of refraction squared.[12-20] This gives a better approximation of the sound speed profile and the eigenfunctions are Airy functions. However, the effects of compressional attenuation of all water and sediment layers is not included in any of the existing models.

Many theoretical[21-37] and experimental[38-54] scientists have shown the importance of attenuation and shear waves in the calculation of the transmission loss and the study of sound propagation in the ocean. Low frequency compressional and shear waves are less attenuated in all layers, so they can penetrate large depths and distances of the ocean. In view of the current interest in low frequency, active and passive sonar systems, it is desirable to extend the Normal Mode theory (which is an exact method

throughout, but is most easily applicable to the low frequency case where the number of modes is small) to the situation of an environment containing range dependence, absorption in all the layers of the media, and birefringence effects due to a shear speed differing from compressional speed on the solid bottom sediments. Assuming high frequencies, the very graphic techniques of acoustic ray tracing have become the standard tools for transmission studies in the deep ocean. However, the more exact, but less graphic, normal mode theory is particularly suited to low frequency propagation in a shallow ocean. Normal mode calculations at higher frequencies are also possible whenever computer time and memory are available.

The formalism to be developed will be based on an existing normal mode propagation model for a range dependent environment.[12-20] This model admits general depth and range dependent sound velocity profiles and an arbitrary but gradual range dependence of a layered ocean bottom containing sound velocity gradients. Sound penetration into the bottom is accounted for by considering not only the modes trapped in the water column but also a sufficiently large number of radiating modes. The set of radiating modes, which is in principle continuous, is discretized by a basement layer of large but finite thickness. For a range-dependent environment, a set of coupled range equations (one for each mode) is obtained which is solved by diagonalization procedures. The algorithm includes absorption in the basement as a first order perturbation to the problem and it ignores the shear waves created in the solid sediments of the bottom.

It is intended here to upgrade this existing model first by taking into account the compressional attenuation coefficient of *all* the layers of the medium and to provide a detailed derivation of the coupled-mode theory.

Eventually, in a next report, the generation and propagation of shear waves, with the effects of its absorption, in the bottom sediments will be included to perform quantitative studies on the effects of absorption and shear waves in the propagation of sound in the water and bottom of a range-dependent stratified ocean. It has been shown that the exact treatment of shear waves in models such as the parabolic equation (PE) approximation is not possible.[55,56]

Absorption effects will be accounted for as a first and second order perturbation to the simpler problem of propagation in a non-absorbing environment instead of using complex sound speed profiles, leading to complex eigenvalues and eigenfunctions since this will necessitate a transition from real to complex Airy functions as the depth function solutions in each layer.[57] Including absorptive effects will not only make it possible to simulate more realistic ocean environments but it will also lead to a more satisfactory procedure for discretizing the continuous distribution of radiating modes.[58]

CHAPTER 2

THEORY

2.1 DERIVATION OF THE WAVE EQUATION FOR FLUID LAYERS

The wave equation is a mathematical description of the reaction of the media due to a disturbance from an external force caused by a source or sources. The media can well be a gas, liquid, or a solid, and the source may be electromagnetic or mechanical. In this report, the mechanical (acoustic) propagation of the disturbance in a fluid media is treated. The fluid media is the ocean environment modeled as a horizontally stratified acoustic waveguide were the surface is treated as a pressure-release (resilient) boundary and the bottom is taken as sediment layers with variable sound speed, density, and attenuation coefficient. The effects of bottom shear waves are neglected even though their importance is well understood and documented in books as the ones in References 59 to 62. Shear wave and its attenuation coefficient will be included to these calculations in a future report.

The disturbance created by the acoustic source may be expressed as a change in the total pressure, relative to the undisturbed pressure, as a function of the density fluctuation created by this external force. If the density fluctuation is much smaller than the undisturbed density of the environment, then the total disturbed pressure may be expanded in the following Taylor series:

$$P(\rho) = P_0 + \left[\frac{\partial P}{\partial \rho}\right]_{\rho_0} (\rho-\rho_0) + \frac{1}{2}\left[\frac{\partial^2 P}{\partial \rho^2}\right]_{\rho_0} (\rho-\rho_0)^2 + \ldots \quad (1)$$

where the partial derivatives are constants determined for the adiabatic compression and expansion of the fluid about its equilibrium density ρ_0, the equilibrium pressure is P_0, and the instantaneous total density is ρ.

If the magnitude of the condensation is much smaller than unity, i.e.

$$s = (\rho - \rho_0)/\rho_0 = \rho_\sim/\rho_0 \quad (2)$$

then then first two terms in the Taylor expansion are of greatest contribution and an acoustic pressure caused by the disturbance may be defined as

$$p = P(\rho) - P_0 \cong \left[\frac{\partial P}{\partial \rho}\right]_{\rho_0} \rho_\sim \quad (3)$$

where by thermodynamic arguments it is found that in an adiabatic media the sound speed is given by

$$c^2 = \left[\frac{\partial P}{\partial \rho}\right]_{\rho_0} \quad (4)$$

and the adiabatic bulk modulus is given by

$$B = \rho_0 c^2 \quad (5)$$

therefore, the acoustic pressure is simplified to

$$p \simeq c^2 \rho_\sim \quad (6)$$

which is called the equation of state.

An equation for the motion of the particles in the fluid is also necessary for the proper environmental description. Consider an infinitesimal cubic volume in the media where the disturbance is taking place as shown in Figure 2(a) for the one-dimensional derivation in cartesian coordinates. Equating forces in a continuous medium gives

$$F_{external} + A\,[P(x) - P(x+dx)] = \frac{d}{dt}(\rho\, A\, dx\, \frac{dx}{dt}) \tag{7}$$

where the external force is the disturbance created by the sound source and can be written in terms of a "force density" with the expression

$$F_{external} = X_e\, A\, dx \tag{8}$$

and using the definition of a derivative

$$\frac{\partial P}{\partial x} = \frac{P(x+dx) - P(x)}{dx} \tag{9}$$

Equation (7) becomes

$$X_e - \frac{\partial P}{\partial x} = V_x \frac{\partial}{\partial x}(V_x \rho) + \frac{\partial}{\partial t}(V_x \rho) \tag{10}$$

which in three dimensions is given by

$$X_e - \vec{\nabla} P = \vec{V}\,(\vec{\nabla} \cdot \rho \vec{V}) + \frac{\partial}{\partial t}(\rho \vec{V}) \tag{11}$$

where the density is a time and space function and the equation is in a non-linear form. The total pressure is P and the total instantaneous particle velocity is $\vec{V}$. Dividing the instantaneous density, pressure, and particle velocity into an undisturbed part and an acoustic part Equation (11) simplifies to the linear form

$$\vec{\nabla} p + \rho_0 \frac{\partial \vec{v}}{\partial t} \simeq X_e \tag{12}$$

where the undisturbed density of the medium is ρ_0, the acoustic pressure is p, and the particle velocity is $\vec{v}$.

Since the fluid of interest is continuous throughout the infinitesimal volume, Figure 2(b) will be helpful in deriving a continuity equation under the argument that the continuous mass going into the volume, $\rho(x)\, A\, V_x(x)\, dt$, must be the same as the quantity going out, $\rho(x+dx)\, A\, V_x(x+dx)\, dt$. There may be an change in mass inside the volume due to the compressibility of the fluid, $\frac{\partial \rho}{\partial t} A\, dx\, dt$, and there may exist a source of mass inside the volume represented by $Q\, A\, dx\, dt$. Taking the definition of the derivative in Equation (9) gives

$$- \frac{d}{dx}(\rho\vec{V})\ A\ dx\ dt = \frac{\partial \rho}{\partial t}\ A\ dx\ dt + Q\ A\ dx\ dt \tag{13}$$

which is rewritten in three dimensions as

$$\vec{\nabla} \cdot (\rho\vec{V}) + \frac{\partial \rho}{\partial t} + Q = 0 \tag{14}$$

or in a linearized form as

$$\rho_0 \vec{\nabla} \cdot \vec{v} + \frac{\partial \rho}{\partial t} = 0 \tag{15}$$

where Q=0 for the sources of interest.[63]

Substituting Equation (6) into Equation (15) for the acoustic density, taking its partial derivative in time, and dropping the subscript 0 of the undisturbed density of the medium, gives

$$\rho \frac{\partial}{\partial t}(\vec{\nabla}\cdot\vec{v}) + c^{-2} \frac{\partial^2}{\partial t^2} p = 0 \tag{16}$$

and taking the divergence of Equation (12) yields

$$\rho\vec{\nabla}\cdot(1/\rho\ \vec{\nabla}p) + \rho \frac{\partial}{\partial t}(\vec{\nabla}\cdot\vec{v}) = \rho\ \vec{\nabla}\cdot(\vec{X}/\rho) \tag{17}$$

which subtracted from Equation (16) provides the inhomogeneous wave equation

$$\rho\vec{\nabla}\cdot(1/\rho\ \vec{\nabla}p) + k^2 p = \rho\ \vec{\nabla}\cdot(1/\rho\ \vec{\nabla}U) \tag{18}$$

where the external force has been written in terms of an external potential energy, time harmonic behavior has been assumed where $k=\omega/c$, and the undisturbed density of the fluid is taken as space dependent. This equation can also be written as

$$\nabla^2 p + k^2 p - \rho^{-1}(\vec{\nabla}\rho)\cdot(\vec{\nabla}p) = \nabla^2 U - \rho^{-1}(\vec{\nabla}\rho)\cdot(\vec{\nabla}U) \tag{19}$$

which is simplified under the change of variables[64]

$$p = \sqrt{\rho}\ \Pi \tag{20}$$

and

$$U = \sqrt{\rho}\ \nu \tag{21}$$

to obtain

$$\nabla^2\Pi + (k^2+K^2)\Pi = \nabla^2\nu + K^2\nu \tag{22}$$

where

$$K^2 = \frac{1}{2\rho}\nabla^2\rho - \frac{3}{4}\left(\frac{1}{\rho}\vec{\nabla}\rho\right)^2. \tag{23}$$

If the density is taken as a linear function of depth, then Equation (23) simplifies. However, the inhomogeneous equation to solve also has a depth dependent wavenumber to worry about due to the depth dependence of the sound speed. The changes in density with depth hardly occurs compared to the changes in sound speed. It is concluded that, for simplicity, the ocean environment can be divided into horizontal layers with constant density. It is understood that the bottom sediments may have layers of large density gradients. In this case, Equation (22) must be solved. In this report, however, layers of constant density are assumed. Then Equation (18) becomes

$$\nabla^2 p + k^2 p = \nabla^2 U \tag{24}$$

which, in an unbounded medium, has a general homogeneous solution consisting of an outgoing and an incoming wave, and an inhomogeneous solution caused by the external force. Since a sound source in a fluid can only produce a scalar potential (no shear waves), the curl of Equation (12) takes us to the property that

$$\vec{\nabla}\times\vec{v} = \text{constant} = \text{vorticity} \tag{25}$$

the vorticity in the media does not change. Therefore, if initially their has been no rotational component of the particle velocity then the vorticity will always be null and this particle velocity can be written in terms of a velocity potential

$$\vec{v} = \vec{\nabla}\varphi \tag{26}$$

which substituted back in Equation (12) gives

$$p = -\rho\frac{\partial\varphi}{\partial t} \tag{27}$$

and assuming harmonic time dependence yields

$$p = -i\omega\rho\,\varphi \tag{28}$$

or

$$\vec{v} = \frac{-i\vec{\nabla}p}{\omega\rho} \quad . \tag{29}$$

Substitution of Equation (28) into Equation (24) provides the inhomogeneous Helmholtz equation

$$\nabla^2\varphi + k^2\varphi = \frac{i}{\omega\rho}\nabla^2 U \tag{30}$$

which must be solved for the velocity potential. If the medium is bounded, then the solution must satisfy the appropriate boundary conditions.

The conservation of energy is obtained by dotting Equation (12) with the particle velocity and substituting the continuity equation, Equation (15), giving the conservation law

$$\frac{\partial \mathcal{E}}{\partial t} + \vec{\nabla}\cdot\vec{I} = 0 \tag{31}$$

where

$$\mathcal{E} = \frac{1}{2}\rho v^2 + \frac{p^2}{2\rho c^2} \tag{32}$$

is the acoustic energy density, and

$$\vec{I} = p\,\vec{v} \tag{33}$$

is the acoustic energy flux or acoustic intensity. Integrating Equation (31) throughout a volume in the fluid medium provides the power

$$\Pi = \frac{d}{dt}\int_V \mathcal{E}\, dV = -\oint_S \vec{I}\cdot\hat{n}\, dS \tag{34}$$

in terms of a closed surface integral around the volume where all the energy is contained.

To obtain these important measurable quantities, it is necessary to solve Equation (30) for the velocity potential. To solve this equation by separation of variables, it has been proven that the sound speed must be function of one variable.[58] This variable is taken to be the vertical direction since temperature and the total pressure of the ocean highly

dependence on depth. A simplified version of Wilson's formula for the sound speed as a function of temperature, salinity, and depth is given by

$$c(z) = 1492.9 + 3(T-10) - 6\times10^{-3}(T-10)^2 - 4\times10^{-2}(T-18)^2 + 1.2(S-35) - 10^{-2}(T-18)(S-35) + z/61 \qquad (35)$$

where the temperature T is in celsius, the salinity S is in parts per thousand, and the depth z is in meters. The formula is accurate to 0.1 m/s for a temperature less than 20°C and for depths less than 8.0 kilometers.[65] Range dependence of the sound speed, density, and position of the boundaries are taken care of by the coupled normal-mode method in Sections 2.6, 2.7, and 2.8 of this report.

2.2 SOLVING THE WAVE EQUATION

It has been found that, in the liquid layers, the inhomogeneous Helmholtz equation

$$[\nabla^2 + k^2(\vec{r})]\ \varphi = \frac{i}{\omega\ \rho}\ \nabla^2 U \tag{36}$$

must be solved, where the sound speed is assumed to be a function of depth only.

In the case of a point source, Equation (36) may be written as

$$[\nabla^2 + k^2(\vec{r})]\ \varphi = -\ S\ \delta(\vec{r} - \vec{r}_o) \tag{37}$$

where S contains all the constants in the inhomogeneous term and is usually called the source strength. For simplicity and without loss of generalization we may set $S = 1$ corresponding to a unitary source strength, then in cylindrical coordinates the equation becomes

$$\left[\frac{1}{r}\frac{\partial}{\partial r}\left(r\frac{\partial}{\partial r}\right) + \frac{\partial^2}{\partial z^2} + k^2(z)\right]\ \varphi(r,z) = -\frac{1}{2\pi r}\ \delta(r)\ \delta(z - z_o) \tag{38}$$

where the source is at $r = 0$, $z = z_o$, and the wavenumber is taken to be depth dependent only since the sound speed must be a function of one variable.[58]

Substituting the Fourier-Bessel transformation,

$$\varphi(r,z) = \int_0^\infty u(k,z)\ J_0(kr)\ k\ dk, \tag{39}$$

$$u(k,z) = \int_0^\infty \varphi(r,z)\ J_0(kr)\ r\ dr, \tag{40}$$

the closure relation,

$$\delta(r - r') = r\int_0^\infty J_0(kr)\ J_0(kr')\ k\ dk, \tag{41}$$

the Bessel equation,

$$k^2r^2\, J_0''(kr) + kr\, J_0'(kr) + k^2r^2\, J_0(kr) = 0, \tag{42}$$

and

$$\frac{\partial}{\partial r}\left(r\, \frac{\partial}{\partial r} \right) J_0(kr) = k\, J_0'(kr) + k^2 r\, J_0''(kr) = -k^2 r\, J_0(kr) \tag{43}$$

into Equation (38) leads us from a partial differential equation to the ordinary differential equation

$$\left[\frac{d^2}{dz^2} + k^2(z) - k^2 \right] u(k,z) = -\frac{\delta(z - z_0)}{2\pi} \tag{44}$$

where k^2 is the eigenvalue and $u(k,z)$ is the eigenfunction of the inhomogeneous equation. After solving for $u(k,z)$, we can transform back using Equation (39) to obtain $\varphi(r,z)$. The solution of this inhomogeneous equation can be written as the sum of the homogeneous solution and the particular or transient solution. The generalized homogeneous solution can be used as the solution of Equation (38). The solution of Equation (39), however, is different since the shear speed and compressional speed of a sediment are usually unequal.

Since the bottom of the oceanic waveguide is not rigid nor resilient, its energy spectrum will contain discrete modes and a continuous distribution which represent the energy that radiates to infinity. The constant wavenumber of the bottom basement represents the dividing point between the continuous and discrete modes. It is possible, however, to discretize the k^2 spectrum by adding to the problem a false resilient boundary. In this case, the homogeneous equation to solve becomes

$$\left[\frac{d^2}{dz^2} + k^2(z) - k_n^2 \right] u_n(z) = 0 \tag{45}$$

where $n = 1,2,\ldots,N$ is the mode index. This false bottom must be deep enough to make the discretized radiative modes very close to each other and better simulate the continuous spectrum. Also it has to be highly absorptive to

avoid reflections of the modes with the false bottom. Since the Earth is not flat, a false resilient bottom satisfying the above conditions is an approximation as good as the assumption of a semi-infinite basement or that of a rigid false bottom.

From the continuity of pressure in the liquid layers, from Section 2.3, we shall set the function $\sqrt{\rho(z)}\ u_n(z)$ as the orthonormal eigenfunctions,

$$\int \rho(z)\ u_n^*(z)\ u_m(z)\ dz = \delta_{nm} \tag{46}$$

with the closure relation

$$\delta(z - z_0) = \rho(z_0) \sum_{n=1}^{N} u_n(z)\ u_n^*(z_0), \tag{47}$$

and the eigenfunction is given by

$$u(k,z) = \sum_{n=1}^{N} a_n(k)\ u_n(z). \tag{48}$$

The inhomogeneous term is taken into account if we substitute the homogeneous solution in the inhomogeneous equation. The substitution gives

$$\left[\frac{d^2}{dz^2} + k^2(z) - k^2 \right] \sum_{n=1}^{N} a_n(k)\ u_n(z) = - \frac{\rho(z_0)}{2\pi} \sum_{n=1}^{N} u_n(z)\ u_n^*(z_0) \tag{49}$$

and substituting the homogeneous equation we get

$$\sum_{n=1}^{N} \left[a_n(k)\ (k^2 - k_n^2) - \frac{\rho(z_0)}{2\pi}\ u_n^*(z_0) \right] u_n(z) = 0 \tag{50}$$

and to satisfy the equation we must set the terms inside the brackets to zero leading to

$$a_n(k) = \frac{\rho(z_0)}{2\pi} \frac{u_n^*(z_0)}{k^2 - k_n^2} \tag{51}$$

which substituted into Equation (52) gives

$$u(k,z) = \frac{\rho(z_0)}{2\pi} \sum_{n=1}^{N} \frac{u_n^*(z_0)\, u_n(z)}{k^2 - k_n^2} \tag{52}$$

and this substituted into Equation (44) gives the scalar potential

$$\varphi(r,z) = \frac{\rho(z_0)}{2\pi} \sum_{n=1}^{N} u_n^*(z_0)\, u_n(z) \int_0^{\infty} \frac{J_0(kr)\, k\, dk}{k^2 - k_n^2} \tag{53}$$

where the integral of this equation is better solved by contour integration and we may define it as

$$I_n(r) = \frac{1}{2} \int_0^{\infty} \frac{H_0^{(1)}(kr) + H_0^{(2)}(kr)}{k^2 - k_n^2}\, k\, dk. \tag{54}$$

A property of the eigenvalues of the problem is that these have a very small imaginary part compared to the real part. Also, both parts of the eigenvalues are positive. This is because we consider only outgoing waves from the source. To solve the integral we can consider contour integration in the first quadrant of the complex k-plane. Consider the contour path displayed in Figure 3, where

$$I_{ni}(r) = \begin{cases} \displaystyle\int_{c_{1i}} \frac{H_0^{(1)}(kr)}{k^2 - k_n^2}\, k\, dk, & i = 1,2,3 \\ \displaystyle\int_{c_{2i}} \frac{H_0^{(2)}(kr)}{k^2 - k_n^2}\, k\, dk, & i = 4,5,6 \end{cases} \tag{55}$$

and, by this definition, the integral we want to solve is,

$$I_{ni}(r) = \frac{1}{2} \left[I_{n1}(r) + I_{n4}(r) \right]. \tag{56}$$

By Jordan's lemma[63] we have that

$$I_{n2}(r) = I_{n5}(r) = 0 \tag{57}$$

also the integrals in Equation (55) show that

$$I_{n3}(r) + I_{n6}(r) = 0 \tag{58}$$

which means that we may write

$$I_n(r) = \frac{1}{2}\left[\sum_{i=1}^{3} I_{ni}(r) + \sum_{i=4}^{6} I_{ni}(r)\right] = \frac{1}{2}\sum_{i=1}^{6} I_{ni}(r) \tag{59}$$

where only $I_{n1}(r)$ and $I_{n4}(r)$ contribute to the sum.

Given that the singularities, $k = k_n$, are located in the upper contour we get that

$$\sum_{i=4}^{6} I_{ni}(r) = \oint_{C_2} \frac{H_0^{(2)}(kr)}{k^2 - k_n^2}\, k\, dk = 0 \tag{60}$$

and

$$\sum_{i=1}^{3} I_{ni}(r) = \oint_{C_1} \frac{H_0^{(1)}(kr)}{k^2 - k_n^2}\, k\, dk = \pi\, i\, H_0^{(1)}(k_n r) \tag{61}$$

by calculus of residues. Substituting Equations (60) and (61) in Equation (59) and this one into Equation (53) gives

$$\varphi(r,z) = \frac{i}{4}\,\rho(z_0) \sum_{n=1}^{N} u_n^*(z_0)\, u_n(z)\, H_0^{(1)}(k_n r) \tag{62}$$

where the eigenfunctions $u_n(z)$, and eigenvalues k_n, satisfy Equation (45). Note that the solution can be written as a separation of variables. Figure 4 shows a qualitative picture of the shape of the modes for several sound speed profiles.

Now we must solve the characteristic equation for the compressional waves, Equation (45). We may start by dividing the sound speed profile into layers where the squared of the index of refraction is a linear function of depth, or

$$n^2(z) = a\, z + b \tag{63}$$

where $k(z) = \omega\, n(z)$ and Figure 5 gives the geometry to be used for this investigation. To determine a and b we let the sound speed at the top of the layer to be c_t and that of the bottom to be c_b. Substituting into our linear equation gives

$$\frac{1}{c_t^2} = a\, z_t + b, \tag{64}$$

and

$$\frac{1}{c_b^2} = a\, z_b + b, \tag{65}$$

which solved for a and b results in

$$a = \frac{c_t^2 - c_b^2}{\ell\, c_t^2\, c_b^2} \tag{66}$$

and

$$b = \frac{1}{c_b^2} - \frac{z_t(c_t^2 - c_b^2)}{\ell\, c_t^2\, c_b^2} \tag{67}$$

where $\ell = z_b - z_t$ is the thickness of the layer. If we define the indices of refraction $n_t^2 = 1/c_t^2$, $n_b^2 = 1/c_b^2$, and $\sigma = (n_t^2 - n_b^2)/\ell$, then we have

$$k^2(z) = \omega^2\left[\, n_t^2 + \sigma\,(z_t - z)\right] = k_t^2 + S\,(z - z_t) \tag{68}$$

where $S = \Delta k^2/\Delta z$, and which substituted into our eigenequation gives

$$\frac{d^2}{dz^2}\, u_n(z) + \left[\, k_t^2 + S\,(z - z_t) - k_n^2 \,\right] u_n(z) = 0. \tag{69}$$

Define

$$\zeta(z) = -|S|^{-2/3}\left[\, k_t^2 + S\,(z - z_t) - k_n^2 \,\right] \tag{70}$$

and square its derivative to obtain

$$\frac{d^2}{dz^2} = |S|^{2/3}\,\frac{d^2}{d\zeta^2} \tag{71}$$

which substituted into the new eigenequation gives

$$\left[\frac{d^2}{d\zeta^2} - \zeta \right] u_n(\zeta) = 0. \tag{72}$$

The solutions of this differential equation are the Bessel functions of order 1/3, or more commonly known as the Airy functions, i.e.

$$u_n(\zeta) = a_n \, Ai(\zeta) + b_n \, Bi(\zeta). \tag{73}$$

The behavior of these functions and their derivative is shown in Figure 4. Now that the general solutions are found, we must match the solutions at each boundary with the appropriate boundary conditions in order to find the unknown coefficients and eigenvalues for each mode.

2.3 DEPTH BOUNDARY CONDITIONS

2.3.1 Boundary Between Fluid Layers

The boundary conditions for the interface between two fluid layers are obtained when an infinitesimal cylindrical volume is modeled across this boundary. In this case we have to satisfy two boundary conditions.

2.3.1.1 Continuity of the Normal Particle Velocity. The volume integration of Equation (15) in this infinitesimal cylinder provides the expression

$$\rho \oint \vec{v} \cdot \hat{n} \, dA = - \frac{\partial}{\partial t} \int \rho \, dA \, \Delta x \tag{74}$$

where making $\Delta x \longrightarrow 0$, the right hand side of the equation vanishes and the surface integral yields the boundary condition

$$\vec{v}_2 \cdot \hat{n} \Big|_s = \vec{v}_1 \cdot \hat{n} \Big|_s . \tag{75}$$

This boundary condition is expressed as $\vec{v} \cdot \hat{n}$ = continuous, and in the case of stratified layers we may write $\hat{n} = \hat{z}$ to obtain the boundary condition,

$$v_z = \frac{\partial \varphi}{\partial z} = \text{continuous} \tag{76}$$

or using Equation (62) we get

$$\frac{du_n}{dz} = \text{continuous}. \tag{77}$$

2.3.1.2 Continuity of the Pressure. Assuming that there is no source in the infinitesimal volume of this cylinder, the volume integration of Equation (12) gives

$$- \oint p \, \hat{n} \, dA = \rho \frac{\partial}{\partial t} \int \vec{v} \, dA \, \Delta x \tag{78}$$

and letting $\Delta x \longrightarrow 0$ yields the pressure boundary condition

$$p_1|_s = p_2|_s \tag{79}$$

where substituting Equation (62) into Equation (28) and this one into Equation (79) gives

$$\rho\, u_n = \text{continuous}. \tag{80}$$

2.3.2 The Resilient Boundary of a Fluid

As a very good approximation, we may consider this boundary as pressure release for acoustic waves in the liquid layer. Therefore, the only boundary condition is that the pressure vanishes at this boundary, i.e.

$$u_n|_{z_0} = 0. \tag{81}$$

2.3.3 Down-Layer Matching Algorithm

Now that the boundary conditions are determined, a matching algorithm is next to by determined. The normalization constant for the eigenfunctions are given by the expression

$$N_n^{-2} = \sum_{j=1}^{J+1} \rho_j \int_{z_j}^{z_{j+1}} |\hat{u}_{nj}|^2 dz \tag{82}$$

where $\hat{u}_{nj}$ is the unnormalized eigenfunction and

$$u_{nj}(z) = N_n \hat{u}_{nj}(z) \tag{83}$$

is the normalized one. For simplicity we will make some further definitions:

$$Ai_{ij} = Ai[\zeta_{ni}(z_j)] \tag{84a}$$

$$Ai'_{ij} = \frac{d\,Ai}{d\zeta_{ni}}\bigg|_{\zeta_{ni}(z_j)} \tag{84b}$$

$$a_j = \frac{d\zeta_{nj}}{dz} = -\,|S_j|^{-2/3} S_j = -\,\mathrm{sgn}(S_j)\,|S_j|^{1/3} \tag{84c}$$

$$P_j = k_j^2(z_j) \tag{84d}$$

and

$$b_{nj} = (P_j - k_n^2)/S_j \tag{84e}$$

which converts Equation (70) to the form

$$\zeta_{nj}(z) = a_j(z+b_{nj}). \tag{85}$$

The layering subscript runs from j=1 at the resilient surface, to j=J+1=B at the upper boundary of the basement as shown in Figure 5.

From the resilient boundary condition at the surface of the ocean, Equation (81), we get

$$\hat{u}_{n1}(z_1) = a_{n1}Ai_{11} + b_{n1}Bi_{11} = 0 \tag{86}$$

and if we write

$$a_{n1} = T_{D1}Bi_{11}, \quad b_{n1} = -T_{D1}Ai_{11} \tag{87}$$

then the solution to the first layer is

$$\hat{u}_{n1}(z) = T_{D1}[Bi_{11}Ai(\zeta_{n1}) - Ai_{11}Bi(\zeta_{n1})] \tag{88}$$

where we can arbitrarily set $T_{D1} = \mathrm{sgn}(S_1)$ to ensure a positive slope of the eigenfunction at the top layer of the media.

The value of the derivative of this function at the surface simplifies to

$$\hat{u}'_{n1}(z_1) = T_{D1}[Bi_{11}Ai'_{11} - Ai_{11}Bi'_{11}] \tag{89}$$

where the term inside the brackets is the Wronskian relation[56]

$$W = Ai(\zeta)\, Bi'(\zeta) - Bi(\zeta)\, Ai'(\zeta) = 1/\pi \tag{90}$$

then

$$\hat{u}'_{n1}(z_1) = -T_{D1}\pi^{-1}. \tag{91}$$

Going back to Equation (73) for the boundary at z_2 we get

$$\hat{u}_{n1}(z_2) = a_{n1}Ai_{12} + b_{n1}Bi_{12} \tag{92a}$$

$$\hat{u}_{n2}(z_2) = a_{n2}Ai_{22} + b_{n2}Bi_{22} \tag{92b}$$

$$\left.\frac{d\hat{u}_{n1}}{dz}\right|_{z=z_2} = \alpha_1(a_{n1}Ai'_{12} + b_{n1}Bi'_{12}) \tag{92c}$$

$$\left.\frac{d\hat{u}_{n2}}{dz}\right|_{z=z_2} = \alpha_2(a_{n2}Ai'_{22} + b_{n2}Bi'_{22}) \tag{92d}$$

and using the liquid boundary conditions we obtain

$$\rho_1(a_{n1}Ai_{12} + b_{n1}Bi_{12}) = \rho_2(a_{n2}Ai_{22} + b_{n2}Bi_{22}) \tag{93a}$$

and

$$\alpha_1(a_{n1}Ai'_{12} + b_{n1}Bi'_{12}) = \alpha_2(a_{n2}Ai'_{22} + b_{n2}Bi'_{22}) \tag{93b}$$

or

$$R_{D2}\hat{u}_{n1}(z_2) = a_{n2}Ai_{22} + b_{n2}Bi_{22} \tag{94a}$$

and

$$T_{D2}\hat{u}'_{n1}(z_2) = a_{n2}Ai'_{22} + b_{n2}Bi'_{22} \tag{94b}$$

where $R_{Dj} = \rho_{j-1}/\rho_j$, and $T_{Dj} = \alpha_{j-1}/\alpha_j$, where $j=2,3,\ldots,J$.

In matrix form we write,

$$\begin{bmatrix} R_{D2}\hat{u}_{n1}(z_2) \\ T_{D2}\hat{u}'_{n1}(z_2) \end{bmatrix} = \begin{bmatrix} Ai_{22} & Bi_{22} \\ Ai'_{22} & Bi'_{22} \end{bmatrix} \begin{bmatrix} a_{n2} \\ b_{n2} \end{bmatrix} \tag{95}$$

and solving for a_{n2} and b_{n2} we have

$$\begin{bmatrix} a_{n2} \\ b_{n2} \end{bmatrix} = \pi \begin{bmatrix} R_{D2}\, Bi'_{22}\, \hat{u}_{n1}(z_2) - T_{D2}\, Bi_{22}\, \hat{u}'_{n1}(z_2) \\ T_{D2}\, Ai_{22}\, \hat{u}'_{n1}(z_2) - R_{D2}\, Ai'_{22}\, \hat{u}_{n1}(z_2) \end{bmatrix} \tag{96}$$

or in general

$$\begin{bmatrix} a_{nj} \\ b_{nj} \end{bmatrix} = \pi \begin{bmatrix} R_{Dj}\, Bi'_{jj}\, \hat{u}_{nj-1}(z_j) - T_{Dj}\, Bi_{jj}\, \hat{u}'_{nj-1}(z_j) \\ T_{Dj}\, Ai_{jj}\, \hat{u}'_{nj-1}(z_j) - R_{Dj}\, Ai'_{jj}\, \hat{u}_{nj-1}(z_j) \end{bmatrix} \tag{97}$$

where the values of the eigenfunction and its derivative at the bottom of any

layer have to be determined before the coefficients of the next layer are sought. This solution is good for "normal-range" values of ζ_{nj}.

In the case of large positive values of ζ_{nj} we can substitute a_{nj} and b_{nj} into the general solution and its derivative to obtain the matrix equation

$$\begin{bmatrix} \hat{u}_{nj}(z) \\ \hat{u}'_{nj}(z) \end{bmatrix} = \pi \begin{bmatrix} C_{11} & C_{12} \\ C_{21} & C_{22} \end{bmatrix} \begin{bmatrix} R_{Dj}\, \hat{u}_{nj-1}(z_j) \\ T_{Dj}\, \hat{u}'_{nj-1}(z_j) \end{bmatrix} \tag{98}$$

where

$$C_{11}(\zeta_{nj}) = Bi'_{jj}\, Ai(\zeta_{nj}) - Ai'_{jj} Bi(\zeta_{nj}) \tag{99a}$$

$$C_{12}(\zeta_{nj}) = Ai_{jj}\, Bi(\zeta_{nj}) - Bi_{jj} Ai(\zeta_{nj}) \tag{99b}$$

$$C_{21}(\zeta_{nj}) = Bi'_{jj}\, Ai'(\zeta_{nj}) - Ai'_{jj} Bi'(\zeta_{nj}) \tag{99c}$$

$$C_{22}(\zeta_{nj}) = Ai_{jj}\, Bi'(\zeta_{nj}) - Bi_{jj} Ai'(\zeta_{nj}) \tag{99d}$$

and the Airy functions nearly cancel each other for large ζ_{nj}.

Now that a recurrence relationship has been found for calculating the eigenfunction at the layer j after calculating it at the layer j-1, we are left with the boundary conditions at the basement. This basement will be taken as a layer with constant acoustic parameters since we will make it deeper than the region of interest. This layer is created for the only purpose of discretizing the continuous wavenumber spectrum. However, the eigenfunction at this layer is exponential in shape when the mode is trapped and oscillatory when the mode is a radiating one, hence we must divide the solutions into two cases.

2.3.3.1 Trapped modes ($k_n > k_B$). The eigenfunction at the basement is given by

$$\hat{u}_{nB}(z) = a_{nB} e^{-\gamma_n z} + b_{nB} e^{\gamma_n z} \tag{100}$$

where $\gamma_n^2 = k_n^2 - k_B^2$. We use the boundary condition at $z=z_F$ (resilient) to get

$$b_{nB} = - a_{nB} e^{-2\gamma_n z_F} \tag{101}$$

which substituted into Equation (100) gives

$$\hat{u}_{nB}(z) = 2a_{nB} e^{-\gamma_n z_F} \sinh \gamma_n (z_F - z). \tag{102}$$

2.3.3.2 Radiating modes ($k_n < k_B$). In this case, the eigenfunction becomes

$$\hat{u}_{nB}(z) = a_{nB} \cos(\eta_n z) + b_{nB} \sin(\eta_n z) \tag{103}$$

where $\eta_n^2 = k_B^2 - k_n^2$. With the boundary condition at $z=z_F$ we get

$$b_{nB} = - a_{nB} \cot(\eta_n z_F) \tag{104}$$

which substituted into Equation (103) yields

$$\hat{u}_{nB}(z) = \frac{a_{nB}}{\sin(\eta_n z_F)} \sin \eta_n (z_F - z). \tag{105}$$

Now we may rewrite Equations (102) and (105) as

$$\hat{u}_{nB}(z) = a_{nB} \begin{cases} \sinh \gamma_n (z_F - z), & k_n > k_B \quad \text{(trapped)} \\ \sin \eta_n (z_F - z), & k_n < k_B \quad \text{(radiating)} \end{cases} . \tag{106}$$

Now we use the boundary conditions at the top of the basement to match Equations (93) with Equations (106). From the continuity of pressure we get

$$\rho_J \hat{u}_{nJ}(z_B) = \rho_B a_{nB} \begin{cases} \sinh \gamma_n (z_F - z_B), & k_n > k_B \\ \sin \eta_n (z_F - z_B), & k_n < k_B \end{cases} \tag{107}$$

and from the continuity of the normal particle velocity we obtain

$$a_J \hat{u}'_{nJ}(z_B) = a_{nB} \begin{cases} \gamma_n \cosh \gamma_n (z_F - z_B), & k_n > k_B \\ \eta_n \cos \eta_n (z_F - z_B), & k_n < k_B \end{cases} \tag{108}$$

and dividing the two equations we get the characteristic equation

$$V(k) = \frac{a_J}{\rho_J} \frac{\hat{u}'_{nJ}(z_B)}{\hat{u}_{nJ}(z_B)} + \frac{1}{\rho_B} \begin{cases} \gamma_n \coth(\gamma_n D), & k_n > k_B \\ \eta_n \cot(\eta_n D), & k_n < k_B \end{cases} \tag{109}$$

where $D = z_F - z_B$.

To avoid singularities in searching for the eigenfunctions and eigenvalues lets rewrite Equation (109) for the trapped modes as

$$W_T(k) = \frac{\gamma_n}{a_J} \hat{u}_{nJ}(z_B) + \frac{\rho_B}{\rho_J} \hat{u}'_{nJ}(z_B) \tanh(\gamma_n D) \tag{110}$$

and for the radiating modes as

$$W_R(k) = \frac{\eta_n}{a_J} \hat{u}_{nJ}(z_B) \cos(\eta_n D) + \frac{\rho_B}{\rho_J} \hat{u}'_{nJ}(z_B) \sin(\eta_n D) \tag{111}$$

which is still the function of interest since we are only interested in finding the zeroes of the characteristic equation. If the trail wavenumber equals an eigenvalue, the characteristic equation for that mode becomes null. To search for these eigenvalues, the locally convergent Newton's method is used to converge to the zero of the characteristic equation.[66]

From Equation (107) we get

$$a_{nB} = \frac{\rho_J}{\rho_B} \hat{u}_{nJ}(z_B) \begin{cases} \operatorname{csch} \gamma_n (z_F - z_B), & k_n > k_B \\ \csc \eta_n (z_F - z_B), & k_n < k_B \end{cases} \tag{112}$$

therefore we obtain for the eigenfunction at the basement the expression

$$\hat{u}_{nB}(z) = \rho_J/\rho_B \, \hat{u}_{nJ}(z_B) \begin{cases} \dfrac{\sinh \gamma_n (z_F - z)}{\sinh(\gamma_n D)}, & k_n > k_B \\ \dfrac{\sin \eta_n (z_F - z)}{\sin \eta_n D}, & k_n < k_B \end{cases} . \tag{113}$$

To eliminate any upward-reflected waves that could have been taken care of by a complex wave-number we rewrite the eigenfunctions as

$$\hat{u}_{nB}(z) = \rho_J/\rho_B \, \hat{u}_{nJ}(z_B) \begin{cases} \dfrac{\exp\,[\gamma_n (z_F - z)]}{2 \sinh(\gamma_n D)}, & k_n > k_B \\ \dfrac{\exp[i\eta_n (z_F - z)]}{2i \sin \eta_n D}, & k_n < k_B \end{cases} . \tag{114}$$

where the up-going waves have been explicitly erased from the equations. If we define

$$\Gamma_n = \frac{N_n \rho_J}{2\rho_B} \hat{u}_{nJ}(z_B) \tag{115}$$

the normalized eigenfunction of the trapped mode becomes

$$u_{nB}(z) = \frac{\Gamma_n}{\sinh(\gamma_n D)} \exp[\gamma_n(z_F - z)] \tag{116}$$

and the radiating mode has a real and an imaginary part given by

$$\mathrm{Re}(u_{nB}) = \frac{\Gamma_n}{\sin(\eta_n D)} \sin[\gamma_n(z_F - z)] \tag{117}$$

and

$$\mathrm{Im}(u_{nB}) = \frac{\Gamma_n}{\sin(\eta_n D)} \cos[\gamma_n(z_F - z)]. \tag{118}$$

Since this model of an oceanic waveguide contains no absorption whatsoever, it is easy to visualize, from Equations (113) and (117), that the radiating mode contains half of its energy propagating downwards and the other half is propagating upwards. The imaginary part in Equation (118) represents the absorptive effect from the basement when we artificially erased the up-going wave from the solution. However, absorption is present in all layers of the media and we will include it in Section 2.4.

2.3.4 Up-Layer Matching Algorithm

When the sound speed is strongly upward-refracting over many of the deeper waveguide layers, it was found that better numerical stability was afforded by stopping the downward-propagated solution at some layer D and propagate the solution upward from the basement to layer U=D+1 with the final Wronskian relation coded to match solutions at the D/U layer interface z_U rather than at z_B.

At the resilient "false" bottom the eigenfunction is automatically set to the small value $\hat{u}_{nB}(z_B) = 10^{-25}$ for the radiating modes since it is an

exponential function. For propagating the solution upwards, the boundary conditions at z_B give:

$$\rho_J \hat{u}_{nJ}(z_B) = \rho_B \hat{u}_{nB}(z_B) \tag{119a}$$

and

$$a_J \hat{u}'_{nJ}(z_B) = \gamma_n \hat{u}_{nB}(z_B) \tag{119b}$$

where ζ is undefined in the isospeed basement and it is possible to write

$$\hat{u}_{nJ}(z_B) = \hat{u}'_{nJ}(z_B) \tag{120}$$

and after the substitution of Equation (73), the boundary conditions become

$$a_{nJ}\, Ai_{JB} + b_{nJ}\, Bi_{JB} = R_{UJ}\, \hat{u}_{nB}(z_B) \tag{121a}$$

and

$$a_{nJ}\, Ai'_{JB} + b_{nJ}\, Bi'_{JB} = T_{UJ}\, \hat{u}'_{nB}(z_B) \tag{121b}$$

where

$$R_{Uj} = \rho_{j+1}/\rho_j, \quad j = D,\ldots,J \tag{122a}$$

$$T_{Uj} = a_{j+1}/a_j, \quad j = D,\ldots,J-1 \tag{122b}$$

and

$$T_{UJ} = \gamma_n/a_J. \tag{122c}$$

Solving the two equations for a_{nJ} and b_{nJ}, as done before, in matrix form yields

$$\begin{bmatrix} a_{nJ} \\ b_{nJ} \end{bmatrix} = \pi \begin{bmatrix} R_{UJ}\, Bi'_{JB}\, \hat{u}_{nB}(z_B) - T_{UJ}\, Bi_{JB}\, \hat{u}'_{nB}(z_B) \\ T_{UJ}\, Ai_{JB}\, \hat{u}'_{nB}(z_B) - R_{UJ}\, Ai'_{JB}\, \hat{u}_{nB}(z_B) \end{bmatrix} \tag{123}$$

and generalizing this solution we have

$$\begin{bmatrix} a_{nj} \\ b_{nj} \end{bmatrix} = \pi \begin{bmatrix} R_{Uj}\, Bi'_{jj+1}\, \hat{u}_{nj+1}(z_{j+1}) - T_{Uj}\, Bi_{jj+1}\, \hat{u}'_{nj+1}(z_{j+1}) \\ T_{Uj}\, Ai_{jj+1}\, \hat{u}'_{nj+1}(z_{j+1}) - R_{Uj}\, Ai'_{jj+1}\, \hat{u}_{nj+1}(z_{j+1}) \end{bmatrix} \tag{124}$$

which is the recurrence relation for upward calculations. In the case of a very large positive value of the argument of the Airy function the matrix to solve is

$$\begin{bmatrix} \hat{u}_{nj}(z) \\ \hat{u}'_{nj}(z) \end{bmatrix} = \pi \begin{bmatrix} E_{11} & E_{12} \\ E_{21} & E_{22} \end{bmatrix} \begin{bmatrix} R_{Uj}\, \hat{u}_{nj+1}(z_{j+1}) \\ T_{Uj}\, \hat{u}'_{nj+1}(z_{j+1}) \end{bmatrix} \tag{125}$$

where

$$E_{11}(\zeta_{nj}) = Bi'_{jj+1}Ai(\zeta_{nj}) - Ai'_{jj+1}Bi(\zeta_{nj}) \tag{126a}$$

$$E_{12}(\zeta_{nj}) = Ai_{jj+1}Bi(\zeta_{nj}) - Bi_{jj+1}Ai(\zeta_{nj}) \tag{126b}$$

$$E_{21}(\zeta_{nj}) = Bi'_{jj+1}Ai'(\zeta_{nj}) - Ai'_{jj+1}Bi'(\zeta_{nj}) \tag{126c}$$

$$E_{22}(\zeta_{nj}) = Ai_{jj+1}Bi'(\zeta_{nj}) - Bi_{jj+1}Ai'(\zeta_{nj}) \tag{126d}$$

and to match the up- and down-layer solutions at z_U, the two remaining boundary conditions are applied at j=U:

$$\hat{u}_{nD}(z_U) = R_{UD}\, \hat{u}_{nU}(z_U) \tag{127a}$$

$$\hat{u}'_{nD}(z_U) = T_{UD}\, \hat{u}_{nU}(z_U) \tag{127b}$$

which are combined to obtain

$$\hat{u}_{nD}(z_U)\, \hat{u}'_{nD}(z_U) = \begin{cases} R_{UD}\, \hat{u}_{nU}(z_U)\, \hat{u}'_{nD}(z_U) \\ T_{UD}\, \hat{u}'_{nU}(z_U)\, \hat{u}_{nD}(z_U) \end{cases} \tag{128}$$

or equating them to the equation

$$R_{UD}\, \hat{u}_{nU}(z_U)\, \hat{u}'_{nD}(z_U) = T_{UD}\, \hat{u}_{nD}(z_U)\, \hat{u}'_{nU}(z_U) \tag{129}$$

which is satisfied only if the trail value is an eigenvalue of the acoustic waveguide. Therefore, the up-layer Wronskian or characteristic equation is defined as

$$\mathfrak{W}(k) = R_{UD}\, \hat{u}_{nU}(z_U)\, \hat{u}'_{nD}(z_U) - T_{UD}\, \hat{u}_{nD}(z_U)\, \hat{u}'_{nU}(z_U) \tag{130}$$

which is zero under the condition just mentioned.

2.4 ABSORPTION AS A PERTURBATION

Now we will consider the complex eigenequation,

$$\frac{d^2}{dz^2} u_n(z) + [\kappa^2(z) - \kappa_n^2] u_n(z) = 0 \tag{131}$$

where we redefine the wave-number as $\kappa(z) = k(z) + i\epsilon\alpha(z)$, ϵ is used here to keep track of the effects of every term in the resulting approximate complex eigenequation and it will be set to unity at the end of the calculations, $\alpha(z)$ is the attenuation coefficient in nepers/meter, and $k(z) = \omega/c(z)$. The complex wavenumber in Equation (131) makes the eigenvalues and eigenfunctions complex. If $\alpha(z) \ll k(z)$, then we can use the perturbation method to obtain a more accurate transmission loss. In this case we will write

$$u_n(z) \longrightarrow u_n^{(0)} + \epsilon\, u_n^{(1)} + \epsilon^2 u_n^{(2)} \tag{132}$$

and

$$\kappa_n^2 \longrightarrow \lambda_n^{(0)} + \epsilon\, \lambda_n^{(1)} + \epsilon^2 \lambda_n^{(2)} \tag{133}$$

which substituted in the complex eigenequation gives,

$$\left[\frac{d^2}{dz^2} + k^2(z) + 2i\epsilon k(z)\alpha(z) - \epsilon^2\alpha^2(z) - \lambda_n^{(0)} - \epsilon\lambda_n^{(1)} - \epsilon^2\lambda_n^{(2)}\right]\left(u_n^{(0)} + \epsilon\, u_n^{(1)} + \epsilon^2 u_n^{(2)}\right) \simeq 0 \tag{134}$$

which is an approximation to the complex eigenequation Equation (131) due to the expansions Equations (132), (133).

Combining the ϵ^0 terms of this equation gives the 0^{th} order solution to the problem, or

$$\frac{d^2}{dz^2} u_n^{(0)} + [k^2(z) - \lambda_n^{(0)}] u_n^{(0)} = 0 \tag{135}$$

which is the unperturbed eigenequation that has been solved for the purely real eigenvalues $\lambda_n^{(0)} = k_n^2$ and eigenfunctions $u_n^{(0)} = u_n$. This unperturbed

eigenequation corresponds to Equation (45).

Combining the terms with ϵ^1, which corresponds to the first order perturbation terms, gives

$$\frac{d^2}{dz^2} u_n^{(1)} + [2ik(z)\alpha(z) - \lambda_n^{(1)}] u_n^{(0)} + [k^2(z) - \lambda_n^{(0)}] u_n^{(1)} = 0 \quad (136)$$

where the unperturbed eigenfunctions are normalized by Equation (46), which in the new notation becomes

$$\int_0^{z_b} \rho(z)\, u_n^{(0)}(z)\, u_m^{(0)}(z)\, dz = \delta_{nm} \quad (137)$$

where z_b is the depth of the resilient bottom of the basement.

Multiplying Equation (136) by $\rho u_n^{(0)}$ and integrating yields

$$\int_0^{z_b} \rho u_n^{(0)} \frac{d^2 u_n^{(1)}}{dz^2}\, dz + \int_0^{z_b} \rho u_n^{(0)} [2ik(z)\alpha(z) - \lambda_n^{(1)}] u_n^{(0)} dz + \int_0^{z_b} \rho u_n^{(0)} [k^2(z) - \lambda_n^{(0)}] u_n^{(1)} dz = 0 \quad (138)$$

where using the orthonormality condition of the unperturbed eigenfunctions in the second term of this equation, integrating by parts twice the first term, and using the boundary conditions at every interface to cancel out the surface contributions gives

$$\int_0^{z_b} \rho u_n^{(1)} \frac{d^2 u_n^{(0)}}{dz^2}\, dz + 2i \int_0^{z_b} \rho u_n^{(0)} k(z)\alpha(z) u_n^{(0)} dz + \int_0^{z_b} \rho u_n^{(0)} [k^2(z) - \lambda_n^{(0)}] u_n^{(1)} dz = \lambda_n^{(1)} \quad (139)$$

and with the help of Equation (135) the first and second integrals cancel out giving us the expression

$$\lambda_n^{(1)} = 2i \int_0^{z_b} \rho\, k(z)\, \alpha(z)\, |u_n^{(0)}|^2 dz \quad (140)$$

which is the first order perturbation term for the eigenvalue and its values are purely imaginary.

Now we write the perturbed part of the eigenfunction under the basis of the unperturbed part since this is an orthonormal basis, i.e.

$$u_n^{(1)} = \sum_m A_{nm}\, u_m^{(0)} \tag{141}$$

and substitute in Equation (136) to obtain

$$\sum_m A_{nm}\left[\frac{d^2u_m^{(0)}}{dz^2} + (k^2(z)-\lambda_n^{(0)})u_n^{(0)}\right] + [2ik(z)\alpha(z)-\lambda_n^{(1)}]u_n^{(0)} = 0 \tag{142}$$

then multiply by $\rho u_l^{(0)}$ and integrate as done before. Integration by parts twice cancels a few terms, and the orthonormality condition yields

$$A_{nl} = \frac{2i}{\lambda_n^{(0)} - \lambda_l^{(0)}}\int_0^{z_b} \rho\, k(z)\alpha(z)\, u_n^{(0)}u_l^{(0)}dz \tag{143}$$

which is in terms of the unperturbed eigenfunctions and eigenvalues, is directly proportional to the absorption coefficient, and it is a purely imaginary term.

In the cases of trapped modes, where the imaginary part of the eigenvalues is extremely small, we can rely on the rapid convergence of the perturbation method and forget about a second order perturbation term. When radiating modes are taken into account, we must make sure that the imaginary part of the eigenvalue is much smaller than the real part. We may stop the eigenvalue search when the real part of the eigenvalue is about 50 times larger than the imaginary part, since the higher modes will not propagate very far. Hamilton has estimated that the shear attenuation coefficient is about 200 times higher than the compressional attenuation coefficient, and the shear speed is from 2 to 30 times smaller than the compressional speed.[42,44,47] However, Werby and Tango found that the shear to compressional attenuation coefficient is only of the order of two.[49] Also, Beebe and Holland found this ratio to be of the order of six.[34] Even though there is some disagreement about the attenuation coefficients, it is suspected, from the ratios given here, that the imaginary part of the shear wavenumber may not be as small as the compressional one is. In this case, it

is feasible to attempt to solve the complex eigenequation without the first order perturbation method or try to get a second order perturbation term and find out how large these effects really are.

The approach here is to continue with the second order perturbation which is needed mostly by the trapped modes when shear waves are included and by the radiating modes. The ϵ^2 terms of Equation (136) into a second order equation gives

$$\frac{d^2}{dz^2} u_n^{(2)} + [k^2(z) - \lambda_n^{(0)}] u_n^{(2)} + [2ik(z)\alpha(z) - \lambda_n^{(0)}] u_n^{(1)} = [\alpha^2(z) + \lambda_n^{(2)}] u_n^{(0)} \tag{144}$$

which multiplied by $\rho u_n^{(0)}$ and integrated as done with the first order eigenvalue leads us to the equation

$$\lambda_n^{(2)} = 2i \int_0^z{}^b \rho k(z)\alpha(z) u_n^{(0)} u_n^{(1)} dz - \lambda_n^{(1)} \int_0^z{}^b \rho u_n^{(0)} u_n^{(1)} dz - \int_0^z{}^b \rho \alpha^2(z) |u_n^{(0)}|^2 dz \tag{145}$$

where substituting Equation (141) and the orthonormality condition of the unperturbed eigenfunctions gives

$$\lambda_n^{(2)} = 2i \sum_m A_{nm} \int_0^z{}^b \rho k(z)\alpha(z) u_n^{(0)} u_m^{(0)} dz - \int_0^z{}^b \rho \alpha^2(z) |u_n^{(0)}|^2 dz \tag{146}$$

or with Equation (143) we get the simpler form

$$\lambda_n^{(2)} = \sum_m A_{nm}^2 (\lambda_n^{(0)} - \lambda_m^{(0)}) - \int_0^z{}^b \rho \alpha^2(z) |u_n^{(0)}|^2 dz \tag{147}$$

which is purely real and a much smaller term since it is proportional to α^2.

If we write

$$u_n^{(2)} = \sum_m B_{nm} u_m^{(0)} \tag{148}$$

then Equation (144) becomes

$$\sum_m B_{nm} \frac{d^2}{dz^2} u_m^{(0)} + \sum_m B_{nm}[k^2 - \lambda_n^{(0)}] u_m^{(0)} + \sum_m A_{nm}[2ik\alpha - \lambda_n^{(1)}] u_m^{(0)} = [\alpha^2 - \lambda_n^{(2)}] u_n^{(0)} \tag{149}$$

which multiplied by $\rho u_l^{(0)}$ and integrated using integration by parts and the orthonormality condition reduces the equation to

$$(\lambda_l^{(0)} - \lambda_n^{(0)})\ B_{nl} = \lambda_n^{(1)} A_{nl} - \sum_m A_{nm} A_{lm} \quad , l \neq n \tag{150}$$

which makes B_{nl} purely real and directly proportional to α^2.

We have already assumed layers of constant density in order to simplify the elastic wave equation. Therefore, we may define an element of a G-matrix as

$$G_{nm} = 2i \sum_{j=1}^{J+1} \rho_j \int_{z_j}^{z_{j+1}} k_j(z)\ \alpha_j(z)\ u_{nj}^{(0)}(z)\ u_{mj}^{(0)}(z)\ dz = G_{mn} \tag{151a}$$

and that of an H-vector as

$$H_n = \sum_{j=1}^{J+1} \rho_j \int_{z_j}^{z_{j+1}} \alpha_j^2(z) \left| u_{nj}^{(0)} \right|^2 dz. \tag{151b}$$

Note that all elements of the G-matrix are purely imaginary and symmetric, while those of the H-vector are purely real. These integrals must be evaluated in order to calculate the perturbed parts of the eigenvalues and eigenfunctions.

Now the first order perturbation term of the eigenvalue, Equation (140), becomes

$$\lambda_n^{(1)} = G_{nn} \tag{152}$$

which tells us that the diagonal components of the G-matrix are the first-order perturbation term of the eigenvalues. The second order term, Equation (145), simplifies to

$$\lambda_n^{(2)} = \sum_{l \neq n} \frac{G_{nl}^2}{\lambda_n^{(0)} - \lambda_l^{(0)}} - H_n \tag{153}$$

which substituted into

$$k_n^2 \simeq \lambda_n^{(0)} + \lambda_n^{(1)} + \lambda_n^{(2)} \tag{154}$$

gives the perturbed eigenvalues of the problem. Since $\lambda_n^{(1)}$ is the only contributor to the imaginary part of the eigenvalue, we may define

$$\mathcal{R}_n^2 = \lambda_n^{(0)} + \lambda_n^{(2)} \tag{155}$$

as the real part of the eigenvalue. Then to obtain k_n from Equation (154) we expand its square root as follows:

$$k_n \simeq \mathcal{R}_n \left(1 + \frac{\lambda_n^{(1)}}{\mathcal{R}_n^2} \right)^{1/2} \cong \mathcal{R}_n \left(1 + \frac{\lambda_n^{(1)}}{2\,\mathcal{R}_n^2} \right) = \mathcal{R}_n + \frac{\lambda_n^{(1)}}{2\,\mathcal{R}_n} \tag{156}$$

where we have assumed that $\mathcal{R}_n^2 >> \lambda_n^{(1)}$. Now the imaginary part of the eigenvalue will be defined as

$$\mathcal{I}_n \simeq \frac{\lambda_n^{(1)}}{2\,\mathcal{R}_n} \tag{157}$$

which is the same expression in page 20 of Reference 24 or in Equation (474) of Reference 14 where only first order perturbation has been used. By the same token, the real part is given from Equation (155)

$$\mathcal{R}_n \simeq \sqrt{\lambda_n^{(0)}} + \frac{\lambda_n^{(2)}}{2\sqrt{\lambda_n^{(0)}}} \tag{158}$$

where it is assumed that $\lambda_n^{(2)} << \lambda_n^{(0)}$ and the same power expansion has been used. Equation (157) is a crude approximations made by many, however, and they are avoided by taking the complex square root of Equation (154).

As the first order correction of the eigenfunction, Equation (143) simply becomes

$$A_{nl} = \frac{G_{nl}}{\lambda_n^{(0)} - \lambda_l^{(0)}}, \quad n \neq l \tag{159}$$

and for the second order correction, Equation (150), we get

$$B_{nl} = \frac{-G_{nn}\,G_{nl}}{(\lambda_n^{(0)} - \lambda_l^{(0)})^2} + \sum_{m \neq n} \frac{G_{nm}\,G_{ml}}{(\lambda_n^{(0)} - \lambda_m^{(0)})(\lambda_n^{(0)} - \lambda_l^{(0)})}, \quad n \neq l \tag{160}$$

which substituted into the equation

$$u_n(z) = u_n^{(0)} + \sum_{l \neq n} [A_{nl} + B_{nl}]\, u_l^{(0)} \tag{161}$$

gives a better estimate of the eigenfunction. These perturbation terms are expected to shift the eigenvalues into the first quadrant of the complex plan as displayed in Figure 6 where the maximum value of the real part of the eigenvalues is calculated using the minimum speed in the sound speed profile.

It is left to properly evaluate of the G-matrix and the H-vector in Equations (151). Instead of numerically integrating these equations, it is possible to make use of some properties of the functions contained in the integrands.

In every layer we may write $c_j(z)=c_{Tj}+(z-z_{Tj})g_j$ where the subscript T stands for the value at the top of the layer. Now the real part of the wavenumber may be expanded assuming speed gradients smaller than unity as follows,

$$\begin{aligned} k_j(z)=\omega/c_j(z) &= \frac{\omega}{c_{Tj}-g_j z_{Tj}} \left[1 + \frac{g_j}{c_{Tj}-g_j z_{Tj}}\, z \right]^{-1} \\ &\simeq \frac{\omega}{c_{Tj}-g_j z_{Tj}} \left[1 - \frac{g_j}{c_{Tj}-g_j z_{Tj}}\, z \right] \end{aligned} \tag{162}$$

and if we define $c_{0j} \equiv c_{Tj}-g_j z_{Tj}$, $K_{Tj} \equiv \omega/c_{0j}$, and $M_j \equiv K_{Tj} g_j/c_{0j}$, nen we have

$$k_j(z) \simeq K_{Tj} - M_j z \tag{163}$$

which is linear with depth if the sound speed gradient is smaller than unity.

The attenuation coefficient in Equations (151) is greatly dependent on

the frequency of the source as shown by Urick[63] in the equation

$$\alpha = \frac{0.1\ f^2}{1 + f^2} + \frac{40\ f^2}{4100 + f^2} + 2.75\text{x}10^{-4}\ f^2 \qquad (164)$$

where this absorption coefficient is in decibels per kiloyards and the frequency is in kilohertz. The dependence upon depth is given by the expression

$$\alpha = \alpha_0(1\text{-}1.93\text{x}10^{-3}z) \qquad (165)$$

where α_0 is the attenuation coefficient at the surface of the ocean. This depth dependence is so small that we will take it to be constant along every layer. In this case we may take the attenuation coefficient outside the integrals and leave it inside the summation across the layers.

The eigenfunctions at all the layers, with the exception of the basement, are given by a linear combination of Airy functions as given in Equation (73). To perform the integrations in Equations (151a and b) with this property of the Airy functions we will use Gordon's formulas given as follows,[57,67-68]

$$\int A[a(z+b)]\ B[a(z+b)]\ dz = (z+b)AB - A'B'/a \qquad (166a)$$

$$\int zA[a(z+b)]B[a(z+b)]dz = AB(z^2\text{-}zb\text{-}2b^2)/3 + (A'B+AB')/6a^2 + (2b\text{-}z)A'B'/3a \qquad (166b)$$

$$\int A[a(z+b_1)]\ B[a(z+b_2)]\ dz = \frac{A'B - AB'}{a^2(b_1 - b_2)} \qquad (166c)$$

$$\int zA[a(z+b_1)]B[a(z+b_2)]dz = \frac{2A'B'}{a^4(b_1\text{-}b_2)^2} + \left[z + \frac{2}{a^3(b_1\text{-}b_2)^2}\right]\frac{A'B\text{-}AB'}{a^2(b_1\text{-}b_2)} - \frac{AB(b_1+b_2+2z)}{a^3(b_1\text{-}b_2)^2} \qquad (166d)$$

where

$$A[a(z+b_1)] = a_1 Ai[a(z+b_1)] + b_1 Bi[a(z+b_1)] \qquad (166e)$$

and

$$B[a(z+b_2)]=a_2 Ai[a(z+b_2)]+b_2 Bi[a(z+b_2)] \tag{166f}$$

represent any linear combination of Airy functions as our eigenfunctions are.

Now we have modified Equation (151a) to the form

$$G_{nm}=2i\sum_{j=1}^{J}\rho_j\alpha_j\int_{z_j}^{z_{j+1}}(K_{Tj}-M_j z)\;u_{nj}^{(0)}[a_j(z+\delta_{nj})]\;u_{mj}^{(0)}[a_j(z+\delta_{mj})]dz+G_{nm}^{(B)} \tag{167}$$

where $G_{nm}^{(B)}$ is the contribution from the isospeed basement to be calculated later on in this section. This equation may be rewritten as

$$G_{nm}=2i\sum_{j=1}^{J}\rho_j\alpha_j\;(\;K_{Tj}\;\mathfrak{I}_{nmj}-M_j\;\mathfrak{J}_{nmj})+G_{nm}^{(B)} \tag{168a}$$

where

$$\mathfrak{I}_{nmj}=\int_{z_j}^{z_{j+1}}u_{nj}^{(0)}[a_j(z+\delta_{nj})]\;u_{mj}^{(0)}[a_j(z+\delta_{mj})]dz \tag{168b}$$

and

$$\mathfrak{J}_{nmj}=\int_{z_j}^{z_{j+1}}z\;u_{nj}^{(0)}[a_j(z+\delta_{nj})]\;u_{mj}^{(0)}[a_j(z+\delta_{mj})]dz \tag{168c}$$

are the integrals to be solved analytically.

The diagonal elements of the $\mathfrak{I}$-matrix are solved substituting Equation (166a) into Equation (168b) giving

$$\mathfrak{I}_{nnj}=\left[(z+\delta_{nj})u_{nj}^2(z)-u'^2_{nj}(z)/a_j\right]_{z_j}^{z_{j+1}} \tag{169a}$$

where the superscript (0) has been dropped for simplicity. Equation (166b) is used to evaluate the n=m elements of the $\mathfrak{J}$-matrix giving

$$\mathfrak{J}_{nnj}=\frac{1}{3}\left[(z^2-z\delta_{nj}-2\delta_{nj}^2)u_{nj}^2(z)+u_{nj}(z)u'_{nj}(z)/a_j^2+(2\delta_{nj}-z)u'^2_{nj}(z)/a_j\right]_{z_j}^{z_{j+1}}. \tag{169b}$$

The off-diagonal elements of the $\mathfrak{I}$-matrix is calculated using Equation (166c) and is simplified to the form

$$\mathfrak{I}_{nmj} = \left[\frac{\mathfrak{L}_{nmj}}{\mathfrak{K}_{nmj}}\right]_{z_j}^{z_{j+1}} \tag{169c}$$

where $\mathfrak{K}_{nmj} = a_j^2 (\delta_{nj} - \delta_{mj})$ and $\mathfrak{L}_{nmj} = u'_{nj}(z)\, u_{mj}(z) - u_{nj}(z)\, u'_{mj}(z)$. Finally, Equation (166d) is used to calculate the off-diagonal elements of the $\mathfrak{I}$-matrix to give

$$\mathfrak{I}_{nmj} = \mathfrak{K}_{nmj}^{-2}\left[2u'_{nj}u'_{mj} + (z\mathfrak{K}_{nmj} + 2a_j\mathfrak{K}_{nmj}^{-1})\mathfrak{L}_{nmj} - a_j(\delta_{nj}+\delta_{mj}+2z)u_{nj}u_{mj}\right]_{z_j}^{z_{j+1}} \tag{169d}$$

where $\mathfrak{K}$ and $\mathfrak{L}$ become null for n=m and Equations (169a) and (169b) must be used.

The normalized basement eigenfunction portion is represented by

$$u_{nB}^{(0)}(z) = \rho_J/\rho_B\, u_{nJ}^{(0)}(z_B)\begin{cases} \dfrac{\sinh \gamma_n(z_F - z)}{\sinh(\gamma_n D)}, & k_n > k_B \quad \text{(trapped modes)} \\ \dfrac{\sin \eta_n(z_F - z)}{\sin(\eta_n D)}, & k_n < k_B \quad \text{(radiating modes)} \end{cases} \tag{170}$$

where $D = z_F - z_B$ is the thickness of the basement, $\gamma_n^2 = k_n^2 - k_B^2$, and $\eta_n^2 = k_B^2 - k_n^2$.

For the trapped modes we substitute in the equation

$$G_{nm}^{(B)} = 2i\rho_B\alpha_B\frac{\omega}{c_B}\int_{z_B}^{z_F} u_{nB}^{(0)}(z)\, u_{mB}^{(0)}(z)\, dz \tag{171}$$

the first expression in Equation (170) to yield

$$G_{nn}^{(B)} = \frac{i\rho_J^2\alpha_B\omega\,[u_{nJ}^{(0)}(z_B)]^2}{\rho_B c_B}\left[\gamma_n^{-1}\coth(\gamma_n D) - D\,\mathrm{csch}^2(\gamma_n D)\right] \tag{172a}$$

for n=m and it becomes

$$G_{nm}^{(B)} = \frac{2i\rho_J^2\alpha_B\omega\, u_{nJ}^{(0)}(z_B)\, u_{mJ}^{(0)}(z_B)}{\rho_B c_B(\gamma_m^2 - \gamma_n^2)}\left[\gamma_m\coth(\gamma_m D) - \gamma_n\coth(\gamma_n D)\right] \tag{172b}$$

when $n \neq m$. Both equations simplify to

$$G_{nm}^{(B)} \simeq \frac{2i\rho_J^2\alpha_B\omega\, u_{nJ}^{(0)}(z_B)\, u_{mJ}^{(0)}(z_B)}{\rho_B c_B(\gamma_n + \gamma_m)} \tag{173}$$

when $\gamma_n D$, and $\gamma_m D$ are much greater than unity.

For the radiating modes we must separate the solution to the cases where

n=m and where n≠m. In the first case, Equations (170) and (171) yield

$$G_{nn}^{(B)} = \frac{i\rho_J^2 \alpha_B \omega}{\rho_B c_B} [u_{nJ}^{(0)}(z_B)]^2 \left[D \csc^2(\eta_n D) - \eta_n^{-1} \cot(\eta_n D) \right], \quad n=m \tag{174a}$$

which corresponds to Equation (172a) for the trapped modes, and for the second case we get

$$G_{nm}^{(B)} = \frac{2i\rho_J^2 \alpha_B \omega \, u_{nJ}^{(0)}(z_B) \, u_{mJ}^{(0)}(z_B)}{\rho_B c_B (\eta_m^2 - \eta_n^2)} [\eta_m \cot(\eta_m D) - \eta_n \cot(\eta_n D)] \tag{174b}$$

which is compatible to Equation (172b) for the trapped modes.

But this is not all. We will also have trapped-radiating mode combination. In the case where mode n is trapped and mode m is radiating our equations yield

$$G_{nm}^{(B)} = \frac{2i\rho_J^2 \alpha_B \omega \, u_{nJ}^{(0)}(z_B) \, u_{mJ}^{(0)}(z_B)}{\rho_B c_B (\eta_m^2 + \gamma_n^2)} [\gamma_n \coth(\gamma_n D) - \eta_m \cot(\eta_m D)] \tag{175}$$

which is like a combination of Equation (172b) and Equation (174b). Since the G-matrix is symmetric, we do not have to evaluate the integral where n is a radiating mode and m is a trapped one.

Finally, we also have to evaluate H_n, given by

$$H_n = \sum_{j=1}^{J} \rho_j \alpha_j^2 \int_{z_j}^{z_{j+1}} u_{nj}^2 \left(a_j (z+\delta_{nj}) \right) dz + H_n^{(B)} \tag{176}$$

which by the use of Equation (166a) we get

$$H_n = \sum_{j=1}^{J} \rho_j \alpha_j^2 \, \mathfrak{I}_{nnj} + H_n^{(B)} \tag{177}$$

where $\mathfrak{I}_{nnj}$ is given in Equation (169a) and it is easy to find that

$$H_n^{(B)} = \rho_B \alpha_B^2 \int_{z_B}^{z_F} u_{nB}^2(z) \, dz = (c_B/\omega) \alpha_B G_{nn}^{(B)}. \tag{178}$$

2.5 THE NORMALIZATION FACTOR

The unperturbed eigenfunction must satisfy the orthonormality condition in Equation (46). They automatically satisfy the orthogonality condition when searching for the zeroes of the characteristic equation because this is an implicit property of the eigenequation, Equation (45). However, the eigenfunctions are not automatically normalized because a function which is any constant multiplied by Equation (73) also satisfies Equation (45). Hence, we must solve Equation (82) for the only constant that will normalize the eigenfunctions in Equation (83). This orthonormal eigenfunction will be the unperturbed function that satisfies Equation (135). Since the eigenfunction at the isospeed basement is different from that of the other layers, we will divide Equation (82) into the basement and "Airy" layers contribution

$$N_n^{-2} = \mathbb{B}_n + \mathbb{X}_n \tag{179}$$

where

$$\mathbb{X}_n = \sum_{j=1}^{J} \rho_j \int_{z_j}^{z_{j+1}} \left| a_{nj} \mathrm{Ai}(\zeta_{nj}) + b_{nj} \mathrm{Bi}(\zeta_{nj}) \right|^2 dz \tag{180}$$

is the contribution of all the "Airy" layers, or layers other than the basement, and with the help of Gordon's formula Equation (166a) we obtain

$$\mathbb{X}_n = \sum_{j=1}^{J} \rho_j \left[(z+\delta_{nj}) \hat{u}_{nj}^2 + \alpha_j^{-1} \hat{u}_{nj}'^2 \right]_{z_j}^{z_{j+1}} \tag{181}$$

where α_j and δ_{nj} are defined in Equation (84). The coefficient $\mathbb{B}_n$ is the basement contribution

$$\mathbb{B}_n = \rho_B \int_{z_B}^{z_F} \left| \hat{u}_{nB}(z) \right|^2 dz \tag{182}$$

and after substituting Equation (170) for the eigenfunction and integrating we get

$$B_n = \frac{\rho_J^2 \hat{u}_{nJ}^2(z_B)}{2\rho_B} \begin{cases} \gamma_n^{-1}\coth(\gamma_n D) - D\,\mathrm{csch}^2(\gamma_n D), & k_n > k_B \\ D\csc^2(\eta_n D) - \eta_n^{-1}\cot(\eta_n D), & k_n < k_B \end{cases} \tag{183}$$

which gives us the complete solution for the normalization coefficient in Equation (179).

A question that may have come to the reader's mind is that of the orthonormalization of the perturbed eigenfunction. We have ensured the orthonormalization of the unperturbed eigenfunction. However, when using the perturbation method, do we automatically have orthonormal perturbed eigenfunctions? Direct substitution of Equation (161) into Equation (46) gives

$$\int \rho\, u_n^* u_m\, dz = B_{nm} + B_{mn} + \sum_{l \neq n,m} (A_{ln}^* A_{lm} + B_{ln} B_{lm} + A_{ln}^* B_{lm} + A_{lm} B_{ln}), \quad n \neq m \tag{184}$$

and for the "renormalization coefficient" we get

$$N_n^{-2} = 1 + \sum_{m \neq n} \left(|A_{mn}|^2 + |B_{mn}|^2 \right) \tag{185}$$

which proves that the perturbed eigenfunctions are not orthonormal unless the perturbation coefficients in Equations (159) and (160) are zero. However, we have shown that A_{nl} and B_{nl} are of the order of α and α^2, respectively, which means that the perturbed eigenfunctions are very close to orthonormal. The reason for this behavior of the perturbed eigenfunctions is that the perturbation method is just an approximation to the problem of solving the complex eigenequation with complex solutions and boundary conditions. However, we have found that this correction to the normalization factor

affects the seventh significant digit of the perturbed eigenfunctions and we may simply assume the perturbed eigenfunctions to be orthonormal. The renormalization factor, Equation (185), will be calculated for this report though, but there is no simple way to make the perturbed eigenfunctions purely orthogonal. The Schmidt orthogonalization procedure[69] is extremely time consuming for the small correction to be made. Equation (184) will simply be used to find out how much error is introduced in the calculation when the perturbation method is used instead of solving the complex eigenequation directly.

2.6 MODE-COUPLING FOR RANGE DEPENDENCE

Now that the depth part of the solution has been found, it is next to treat the range part of the solution. Consider the inhomogeneous Helmholtz equation,

$$[\nabla^2 + k^2(r,z)]\ \varphi(r,z) = -\frac{1}{2\pi r}\ \delta(r)\ \delta(z-z_0) \tag{186}$$

where the solution will be written in the almost-separated form

$$\varphi(r,z) = \sum_{n=1}^{N} \Psi_n(r)\ u_n(r,z) \tag{187}$$

which embodies the "adiabatic range-variation" method. The unknown is $\Psi_n(r)$ and the function $u_n(r,z)$ is the n^{th} range-independent eigenfunction at the range segment where r is contained. If $u_n(r,z)$ are taken as the "basis" eigenfunctions that satisfy the equation

$$\frac{\partial^2}{\partial z^2}\ u_n(r,z) + [k^2(r,z) - k_n^2(r)]\ u_n(r,z) = 0 \tag{188}$$

where

$$\int_0^{z_F} \rho(z)\ u_n(r,z)\ u_m^*(r,z)\ dz = \delta_{nm} \tag{189}$$

then the inhomogeneous Helmholtz equation becomes

$$\sum_{n=1}^{N} \left\{ \left[(\nabla_r^2 + k_n^2)\Psi_n\right] u_n + 2\ \vec{\nabla}_r \Psi_n \cdot \vec{\nabla}_r u_n + \Psi_n\ \nabla_r^2 u_n \right\} = -\frac{1}{2\pi r}\ \delta(r)\ \delta(z-z_0) \tag{190}$$

where

$$\nabla_r^2 = \frac{\partial^2}{\partial r^2} + \frac{1}{r}\frac{\partial}{\partial r}\ . \tag{191}$$

Multiply both sides by $\rho(z)\ u_m^*(0,z)$ and integrate to obtain the range equation

$$\left[\frac{d^2}{dr^2} + \frac{1}{r}\frac{d}{dr} + k_n^2(r) \right] \Psi_n(r) = -\frac{1}{2\pi r}\,\delta(r)\,\rho(z_0)\,u_n^*(0,z_0) - 2\sum_m \frac{d\Psi_m}{dr} M'_{nm}(r) - \sum_m \Psi_m(r) M''_{nm}(r) \tag{192}$$

where

$$M'_{nm}(r) = \int_0^{z_F} \rho(z)\,u_m^*(r,z)\,\frac{\partial}{\partial r}\,u_n(r,z)\,dz \tag{193a}$$

and

$$M''_{nm}(r) = \int_0^{z_F} \rho(z)\,u_m^*(r,z)\left[\frac{\partial^2}{\partial r^2} + \frac{1}{r}\frac{\partial}{\partial r} \right] u_n(r,z)\,dz \tag{193b}$$

or

$$M''_{nm}(r) = \frac{1}{r}\,M'_{nm}(r) + V_{nm}(r) \tag{193c}$$

where

$$V_{nm}(r) = \int_0^{z_F} \rho(z)\,u_m^*(r,z)\,\frac{\partial^2}{\partial r^2}\,u_n(r,z)\,dz \tag{193d}$$

are the coupling coefficients of the inhomogeneous equation and these are null when the eigenfunctions have no range dependence. Note that Equation (192) is a set of N equations for $\Psi_n(r)$ coupled in all the depth eigenfunctions. This is the equation to be solved by the coupled normal-mode method. To simplify this equation it is desirable to eliminate the first derivative by introducing a new function defined by

$$\Psi_n(r) = r^{-1/2} f_n(r) \tag{194}$$

which transforms Equation (192) to the form

$$\left[\frac{d^2}{dr^2} + \frac{1}{4r^2} + k_n^2(r)\right] f_n(r) = \frac{-1}{2\pi r^{1/2}}\,\delta(r)\,\rho(z_0)\,u_n^*(0,z_0) - 2\sum_m M'_{nm}(r)\,\frac{df_m}{dr} - \sum_m V_{nm}(r)\,f_m(r) \tag{195}$$

or all N coupled equations can be written in the matrix form

$$\left[\frac{d^2}{dr^2} + \frac{1}{4r^2} + K^2(r)\right] F(r) = U(r) - 2\, M'(r)\, F'(r) - V(r)\, F(r) \qquad (196)$$

where

$$F(r) = \begin{bmatrix} f_1(r) \\ f_2(r) \\ \vdots \\ f_N(r) \end{bmatrix} \qquad (197)$$

and its derivative is the derivative of every element in the matrix. Also we have

$$K^2(r) = \begin{bmatrix} k_1^2(r) & 0 & \cdots & 0 \\ 0 & k_2^2(r) & \cdots & 0 \\ \vdots & \vdots & & \vdots \\ 0 & 0 & \cdots & k_N^2(r) \end{bmatrix} \qquad (198)$$

and

$$U(r) = \frac{-1}{2\pi r^{1/2}}\, \delta(r)\, \rho(z_0) \begin{bmatrix} u_1^*(0,z_0) \\ u_2^*(0,z_0) \\ \vdots \\ u_N^*(0,z_0) \end{bmatrix} \qquad (199)$$

which helps in the simplification of the range equation.

The method consists in dividing the range-dependent environment into range-independent segments where the first segment is the only one with a source and the last one is semi-infinite as qualitatively shown in Figure 7. The coupling will occur in the other segments and the radial boundary conditions are easily satisfied as long as the slope of the bottom is small. Under these assumptions we can simplify the coupled range equation for every segment and find its solutions.

2.6.1 Range Segment Number 1

In this segment we assume range independence and note that this is the only segment containing the omnidirectional source. Under these conditions Equation (196) decouples to form

$$\left[\frac{d^2}{dr^2} + \frac{1}{4r^2} + K^2(r_0)\right] F^{(1)}(r) = U(r) \tag{200}$$

which has the homogeneous solution

$$f_n^{(1)}(r) = r^{1/2}\left[\alpha_n^{(1)} H_0^{(1)}(k_n^0 r) + \beta_n^{(1)} H_0^{(2)}(k_n^0 r)\right] \tag{201}$$

where $k_n^0 = k_n(r_0)$, and the alphas and betas are coefficients to be determined via the radial boundary conditions. The inhomogeneous term U(r) will be taken into account later on when matching the field to the source. For simplicity, this solution can be rewritten as

$$f_n^{(1)}(r) = \left[{}^1H_n(r) \quad {}^2H_n(r)\right] \vec{\alpha}_n^{(1)} \tag{202}$$

where

$$\vec{\alpha}_n^{(i)} = \begin{bmatrix} \alpha_n^{(i)} \\ \beta_n^{(i)} \end{bmatrix} \tag{203}$$

and

$${}^jH_n(r) = r^{1/2} H_0^{(j)}(k_n^0 r) \quad , \; j=1,2. \tag{204}$$

2.6.2 Range Segment Number M+1

In this segment we also assume range independence, but there also is no source. This makes Equation (196) uncoupled and homogeneous. Also, due to its semi-infinite property, we will only accept the radiation solution to the equation

$$\left[\frac{d^2}{dr^2} + \frac{1}{4r^2} + K^2(r_M)\right] F^{(M+1)}(r) = 0 \tag{205}$$

which is

$$f_n^{(M+1)}(r) = r^{1/2}\, \alpha_n^{(M+1)}\, H_0^{(1)}(k_n^M r) \tag{206}$$

where $k_n^M = k_n(r_M)$. For simplicity we can write these functions as elements of the matrix equation

$$F^{(M+1)}(r) = A\, H(r) \tag{207}$$

where

$$H_n(r) = r^{1/2}\, H_0^{(1)}(k_n^M r). \tag{208}$$

2.6.3 Range Segments Number $2 \le i \le M$

These segments are range dependent as a whole and the coupling terms are kept. However, the source term is zero and to simplify the equation we assume these segments to be at a range much larger than a wavelength. Under these assumptions the range equation for these segments become

$$\left[\frac{d^2}{dr^2} + K^2(\bar{r}_i)\right] F^{(i)}(r) + 2\, M'(\bar{r}_i)\, F'^{(i)}(r) + V(\bar{r}_i)\, F^{(i)}(r) = 0 \tag{209}$$

where $\bar{r}_i = (r_{i-1} + r_i)/2$ and the matrices are constant values averaged to be determined at the boundary between every range segment. A series of transformations is next performed in order to repeatedly diagonalize matrices and regroup terms until the modes are uncoupled.

To solve Equation (209) we define S_1 as the range-independent matrix that diagonalizes $M'(\bar{r}_i)$ to have diagonal elements λ_n as follows,

$$\lambda = S_1^{-1} M' S_1 = \begin{bmatrix} \lambda_1 \cdots 0 \\ \vdots \quad \vdots \\ 0 \cdots \lambda_N \end{bmatrix} \tag{210}$$

where $S_1 S_1^{-1} = \mathbb{I}$ is a useful property satisfied by this transformation matrix. If we multiply the left hand side of the range equation by S_1^{-1} then this equation becomes

$$\left[\frac{d^2}{dr^2} + K^2 + W \right] \Gamma(r) + 2 \lambda \Gamma'(r) = 0 \tag{211}$$

where $K^2 = S_1^{-1} K^2(\bar{r}_1) S_1$, $W = S_1^{-1} V S_1$, $\lambda = S_1^{-1} M' S_1$, and $\Gamma(r) = S_1^{-1} F^{(i)}(r)$.

Now we will define

$$\sigma_n(r) = \exp(-\lambda_n r) \tag{212}$$

as the elements of the diagonal matrix $\sigma(r)$, where $\sigma^{-1}\sigma = \mathbb{I}$ is satisfied, and also define

$$\Gamma(r) = \sigma(r)\ \gamma(r) \tag{213}$$

which substituted in the equation gives

$$\left[\frac{\partial^2}{\partial r^2} + K^2 + W \right] \sigma\ \gamma + 2 \lambda\ (\sigma\ \gamma' + \sigma' \gamma) = 0 \tag{214}$$

and now multiply by σ^{-1} to the left to obtain

$$\left[\frac{d^2}{dr^2} + T \right] \gamma(r) = 0 \tag{215}$$

where

$$\begin{aligned} T &= \sigma^{-1} (K^2 + W)\ \sigma - \lambda^2 \\ &= \sigma^{-1}\ S_1^{-1} (K^2 + V) S_1 \sigma - \lambda^2 \end{aligned} \tag{216}$$

and

$$\gamma(r) = \sigma^{-1} S_1^{-1}\ F^{(i)}(r) \tag{217}$$

have simplified the equation considerably, but they are still coupled because T is not diagonal. They are finally uncoupled by finding the matrix S_2 that diagonalizes T to have elements Λ_n with the transformation

$$\Lambda = S_2^{-1}\ T\ S_2 = \begin{pmatrix} \Lambda_1 \cdots 0 \\ \vdots \quad \vdots \\ 0 \cdots \Lambda_N \end{pmatrix} \tag{218}$$

where $S_2 S_2^{-1} = \mathbb{I}$ is satisfied. Multiplying the left hand side of Equation (215)

by S_2^{-1} takes us to the final form

$$\left[\frac{d^2}{dr^2} + \Lambda \right] \mathcal{P}(r) = 0 \tag{219}$$

which has the solutions

$$\mathcal{P}(r) = S_2^{-1}\gamma(r) = \begin{bmatrix} \alpha_1\cos(q_1 r) + \beta_1\sin(q_1 r) \\ \alpha_2\cos(q_2 r) + \beta_2\sin(q_2 r) \\ \vdots \\ \alpha_N\cos(q_N r) + \beta_N\sin(q_N r) \end{bmatrix} \tag{220}$$

where $q_n = \Lambda_n^{1/2}$, and α_n, β_n are the unknown to be determined by the application of the boundary conditions and all superscript (i) indicating the range segment of evaluation has been momentarily dropped for clarity. Taking all the transformations that connect F(r) to $\mathcal{P}(r)$ it is easy to find that

$$F(r) = [S_1\sigma(r)\ S_2]\ \mathcal{P}(r) = \mathcal{U}\ \mathcal{P}(r) \tag{221}$$

or back to the original form we get

$$f_n^{(i)}(r) = \sum_{m=1}^{N} \mathcal{U}_{nm}^{(i)} \left[\alpha_m^{(i)}\cos(q_m^{(i)} r) + \beta_m^{(i)}\sin(q_m^{(i)} r) \right] \tag{222}$$

and

$$F^{(i)}(r) = \mathcal{U}^i\ \mathcal{P}^i(r) \tag{223}$$

where n = 1,2,...,N is the mode index, i = 2,3,...,M is the segment index, $\mathcal{U}$ is not a diagonal matrix, and the unknown coefficients are in $\mathcal{P}^i(r)$. Now that the radial functions have been found, it is next to match them to satisfy the radial boundary conditions.

2.7 THE RADIAL BOUNDARY CONDITIONS

The radial boundary conditions are the same in principle to those for the depth functions. The only difference is in the coordinate used to satisfy for the continuity of pressure and normal particle velocity. Since the range segments are small and a linear fit is used to connect the n^{th} eigenfunction radially, then it is assumed that the eigenfunction and its radial derivative are radially continuous. Substituting Equations (194), (187), and (28) into Equation (79) gives

$$f_n^{(i)}(r_i) = f_n^{(i+1)}(r_i) \tag{224}$$

for the continuity of pressure in the radial direction at the interface r_i.

The next boundary condition is given by taking the radial derivative of the velocity potential

$$\frac{\partial \varphi}{\partial r} = \sum_{n=1}^{N} \left(\frac{d\Psi_n}{dr} u_n + \Psi_n \frac{\partial u_n}{\partial r} \right) \tag{225}$$

where the last three functions in the parenthesis are already continuous and the first function is the one to be satisfied by writing

$$\left. \frac{df_n^{(i)}}{dr} \right|_{r_i} = \left. \frac{df_n^{(i+1)}}{dr} \right|_{r_i} \tag{226}$$

where $i = 1,2,\ldots,M$.

Apply the boundary conditions at r_M to get

$$A\, H(r_M) = \mathcal{U}^M \mathcal{P}^M(r_M) \tag{227a}$$

and

$$A\, H'(r_M) = \mathcal{U}^M \mathcal{P}^{M\prime}(r_M) \tag{227b}$$

where

$$H_n'(r_M) = k_n^M r_M^{-1/2} H_0^{(1)\prime}(k_n^M r_M) - \frac{1}{2} r^{-3/2} H_0^{(1)}(k_n^M r_M) \tag{228}$$

and

$$\mathcal{P}_n^{M\prime}(r_M) = -\alpha_n^M q_n^M \sin(q_n^M r_M) + \beta_n^M q_n^M \cos(q_n^M r_M). \tag{229}$$

To further simplify the calculations, let's define a hyper-space vector as

$$\overleftrightarrow{\alpha}^{(i)} = \begin{bmatrix} \vec{\alpha}_1^{(i)} \\ \vec{\alpha}_2^{(i)} \\ \vdots \\ \vec{\alpha}_N^{(i)} \end{bmatrix} \tag{230}$$

and

$$C_n^j(r_i) = \begin{bmatrix} \cos(q_n^j r_i) & \sin(q_n^j r_i) \\ -q_n^j \sin(q_n^j r_i) & q_n^j \cos(q_n^j r_i) \end{bmatrix} \tag{231}$$

which has the inverse form

$$[C_n^j(r_i)]^{-1} = \begin{bmatrix} \cos(q_n^j r_i) & -\sin(q_n^j r_i)/q_n^j \\ \sin(q_n^j r_i) & \cos(q_n^j r_i)/q_n^j \end{bmatrix} \tag{232}$$

and the hyper-space matrix

$$C^j(r_i) = \begin{bmatrix} C_1^j(r_i) & 0 & \cdots & 0 \\ 0 & C_2^j(r_i) & & \vdots \\ \vdots & & & \\ 0 & \cdots & & C_N^j(r_i) \end{bmatrix} \tag{233}$$

with an inverse given by the inverse of the individual diagonal elements in this matrix. Finally it is helpful to define

$$\vec{H}_n = \begin{bmatrix} H_n(r_M) \\ H_n'(r_M) \end{bmatrix}, \quad n=1,2,\ldots,N \tag{234}$$

and the hyper-space vector

$$\overleftrightarrow{H}_n = \begin{bmatrix} \vec{H}_1 \\ \vec{H}_2 \\ \vdots \\ \vec{H}_N \end{bmatrix} \tag{235}$$

then the matching of the radial functions at r_M becomes,

$$\alpha_n^{(M)}\cos(q_n^{(M)}r_M) + \beta_n^{(M)}\sin(q_n^{(M)}r_M) = \sum_{m=1}^{N}\left[\left(U^{(M)}\right)^{-1}A\right]_{nm} H_m(r_m) \quad (236)$$

and

$$-\alpha_n^{(M)}q_n^{(M)}\sin(q_n^{(M)}r_M) + \beta_n^{(M)}q_n^{(M)}\cos(q_n^{(M)}r_M) = \sum_{m=1}^{N}\left[\left(U^{(M)}\right)^{-1}A\right]_{nm} H'_m(r_m) \quad (237)$$

or in hyper-space matrix form, both equations combine into the equation

$$C_n^{(M)}(r_M)\,\vec{\alpha}_n^{(M)} = \sum_{m=1}^{N}\left[\left(U^{(M)}\right)^{-1}A\right]_{nm}\vec{H}_m \quad (238)$$

or

$$\overleftrightarrow{\alpha}^{(M)} = [C^{(M)}(r_M)]^{-1}[U^{(M)}]^{-1}\,A\,\overleftrightarrow{H} \quad (239)$$

which is a recurrence relation between the last semi-infinite segment and the last finite segment coefficients to be determined.

For the intermediate boundaries, i=2,3,...,M-1, the functions and their derivatives are matched to obtain

$$\mathcal{P}^{(i)}(r_i) = [U^{(i)}]^{-1}\,U^{(i+1)}\,\mathcal{P}^{(i+1)}(r_i) \quad (240)$$

and

$$\mathcal{P}^{(i)\prime}(r_i) = [U^{(i)}]^{-1}\,U^{(i+1)}\,\mathcal{P}^{(i+1)\prime}(r_i). \quad (241)$$

Combining the n^{th} row of each and gathering both sets of equations leads to

$$C_n^{(i)}(r_i)\,\vec{\alpha}_n^{(i)} = \sum_{m=1}^{N}[U^{(i)}]^{-1}\,U^{(i+1)}C_m^{(i+1)}(r_i)\,\vec{\alpha}_m^{(i+1)} \quad (242)$$

and shifting to hyper-space gives

$$\overleftrightarrow{\alpha}^{(i)} = [C^{(i)}(r_i)]^{-1}\,[U^{(i)}]^{-1}\,U^{(i+1)}\,C^{(i+1)}(r_i)\,\overleftrightarrow{\alpha}^{(i+1)}\,,\quad i=2,3,\ldots,M-1 \quad (243)$$

which is the recurrence relation for the unknown coefficients at the finite range segments.

After applying the boundary conditions of the remaining interface and writing both sets into one matrix equation we get

$$\mathcal{H}_n \vec{\alpha}_n^{(1)} = \sum_{m=1}^{N} U_{nm}^{(2)} C_m^{(2)}(r_1) \vec{\alpha}_m^{(2)} \tag{244}$$

where

$$\mathcal{H}_n = \begin{bmatrix} {}^1H_n(r_1) & {}^2H_n(r_1) \\ {}^1H'_n(r_1) & {}^2H'_n(r_1) \end{bmatrix} \tag{245}$$

and in hyper-space notation it is found the third recurrence relation

$$\overleftrightarrow{\alpha}^{(1)} = \mathcal{H}^{-1} U^{(2)} C^{(2)}(r_1) \overleftrightarrow{\alpha}^{(2)} \tag{246}$$

where

$$\mathcal{H}^{-1} = \begin{bmatrix} \mathcal{H}_1^{-1} & 0 & \cdots & 0 \\ 0 & \mathcal{H}_2^{-1} & & \vdots \\ \vdots & & & \\ 0 & \cdots & & \mathcal{H}_N^{-1} \end{bmatrix} \tag{247}$$

is the matrix that uncoupled the source segment coefficients, $\alpha_n^{(1)}$ and $\beta_n^{(1)}$, thus providing them in terms of $\alpha_n^{(2)}$ and $\beta_n^{(2)}$, or ultimately, $\alpha_n^{(M+1)}$. After multiple substitution of the calculated hyper-space equation we get a relationship between the unknown coefficients in the source segment and the unknown coefficient in the semi-infinite segment given by,

$$\overleftrightarrow{\alpha}^{1} = \mathcal{H}^{-1} U^2 C^2(r_1) \prod_{i=2}^{M-1} \left\{ [C^i(r_i)]^{-1} [U^i]^{-1} U^{i+1} C^{i+1}(r_i) \right\} [C^M(r_M)]^{-1} [U^M]^{-1} A \overleftrightarrow{H} \tag{248}$$

where the parenthesis at the superscript have been momentarily eliminated to write the equation in one line. This relationship can be greatly simplified to the form

$$\overleftrightarrow{\alpha}^{(1)} = X A \overleftrightarrow{H} \tag{249}$$

where

$$X = \mathcal{K}^{-1} \prod_{i=2}^{M} \left\{ U^{(i)} C^{(i)}(r_{i-1}) \; [C^{(i)}(r_i)]^{-1} \; [U^{(i)}]^{-1} \right\}. \tag{250}$$

The n^{th} hyper-row is given by

$$\vec{\alpha}^{(1)} = \sum_m X_{nm} \, A_m \, \vec{H}_m \tag{251}$$

where $A_m = \alpha_m^{(M+1)}$, and back out from the matrix notation the coefficients for the first range segment are given by

$$\alpha_n^{(1)} = \sum_m A_m \left(X_{nm}^{11} H_m + X_{nm}^{12} H'_m \right) \tag{252}$$

and

$$\beta_n^{(1)} = \sum_m A_m \left(X_{nm}^{21} H_m + X_{nm}^{22} H'_m \right) \tag{253}$$

where

$$X_{nm} = \begin{bmatrix} X_{nm}^{11} & X_{nm}^{12} \\ X_{nm}^{21} & X_{nm}^{22} \end{bmatrix} \tag{254}$$

and r_M has been dropped.

It is now time to take into consideration the behavior of the source at r=0. This is the last matching to be performed to obtain the necessary number of equations to evaluate all the unknowns in a closed form. In this first segment it was found that the homogeneous solution to the inhomogeneous and uncoupled equation is

$$\Psi_n(r) = \alpha_n^{(1)} H_0^{(1)}(k_n^0 r) + \beta_n^{(1)} H_0^{(2)}(k_n^0 r) \tag{255}$$

and in the limit as $k_n r \longrightarrow 0$ we find that

$$H_0^{(1)}(k_n^0 r) = - H_0^{(2)}(k_n^0 r) \longrightarrow \frac{2i}{\pi} \ln(k_n^0 r) \tag{256}$$

which gives

$$\Psi_n(r) \longrightarrow \frac{2i}{\pi} \left(\alpha_n^{(1)} - \beta_n^{(1)} \right) \ln(k_n^0 r). \tag{257}$$

An asymptotic solution can also be calculated by integrating the uncoupled, inhomogeneous equation over a small cylinder containing the source, and

taking the limit as the radius goes to zero. The procedure gives

$$\int_0^a \frac{d^2\Psi_n}{dr^2}\,dr + \int_0^a \frac{1}{r}\frac{d\Psi_n}{dr}dr + \int_0^a k_n^2(r)\,\Psi_n(r)\,dr = -\frac{\rho(z_0)\,u_n^*(0,z_0)}{2\pi}\int_0^a \frac{\delta(r)}{r}\,dr \tag{258}$$

where the second term is integrated by parts to yield

$$\frac{d\Psi_n}{dr}\Big|_0^a + \frac{\Psi_n}{r}\Big|_0^a + \int_0^a \left[\,r^{-2} + k_n^2(r)\right]\Psi_n(r)\,dr = -\frac{\rho(z_0)\,u_n^*(0,z_0)}{2\pi}\int_0^a \frac{\delta(r)}{r}\,dr \tag{259}$$

and in the limit as $a \longrightarrow 0$ only the slope at r=0 and the integral over the delta function remains providing the expression

$$\frac{d\Psi_n(r)}{dr} \longrightarrow -\frac{\rho(z_0)\,u_n^*(0,z_0)}{2\pi r} \tag{260}$$

or

$$\Psi_n(r) \longrightarrow -\frac{1}{2\pi}\,\rho(z_0)\,u_n^*(0,z_0)\,\ln(k_n^0 r) \tag{261}$$

which can now be equated to the other asymptotic solution providing

$$\alpha_n^{(1)} - \beta_n^{(1)} - i/4\;\;\rho(z_0)\,u_n^*(0,z_0) = V_n \tag{262}$$

which is the relationship between $\alpha_n^{(1)}$ and $\beta_n^{(1)}$. Substitution of the calculated coefficients into this equation gives

$$V_n = \sum_m \left[(X_{nm}^{11} - X_{nm}^{21})\,H_m + (X_{nm}^{12} - X_{nm}^{22})\,H'_m\right] A_m = \sum_m B_{nm} A_m \tag{263}$$

or in matrix form

$$\vec{V} = B\,\vec{A} \tag{264}$$

and after inverting the matrix B (if it is not singular) the first unknowns are obtained with the equation

$$\vec{A} = B^{-1}\vec{V}. \tag{265}$$

After this matrix is calculated, it follows to calculate the unknowns of the source segment with Equations (252) and (262). The coefficients of the other segments are calculated using Equations (239) and (243). Finally, the

range functions are obtained with Equations (201), (206), and (222) where the Hankel functions are calculated with the complex eigenvalues obtained in Section 2.4.

Note that this coupling method is in a closed form that requires no iteration that may slow-down the computation time. It is left to evaluate the coupling coefficients which is done in the next section.

2.8 REDUCING THE COUPLING INTEGRALS

The coupling integrals are given in Equations (193) where the eigenfunctions satisfy Equations (188) and (189). Under the assumptions of an environment that slowly varies with range, it is possible to use Gordon's formulas in Equations (166) to solve the coupling integrals.

The range-dependent environment is divided into range-independent segments as shown in Figure 7. The eigenvalues and eigenfunctions have been calculated for the middle of the segments at r_i. A method of evaluation is to multiply Equation (188) by the operator $\int_0^{z_F} dz\ \rho(z)\ u_m^*(r,z)\ \frac{\partial}{\partial r}$ to yield the expression

$$\int_0^{z_F} \rho u_m^* \frac{\partial}{\partial z}\left[\frac{\partial}{\partial r}\left(\frac{\partial}{\partial z}\ u_n\right)\right] dz + \int_0^{z_F} \rho u_m^* \left(\frac{\partial k^2}{\partial r}\right) u_n\, dz + \int_0^{z_F} \rho u_m^*\ k^2(r,z)\ \frac{\partial u_n}{\partial r}\ dz =$$

$$\int_0^{z_F} \rho u_m^*\ \left(\frac{\partial k_n^2}{\partial r}\right) u_n\, dz + \int_0^{z_F} \rho u_m^*\ k_n^2(r)\ \frac{\partial u_n}{\partial r}\ dz \qquad (266)$$

where $n \neq m$. Since the eigenvalue is independent of depth, the first integral in the right hand side of this equation vanishes due to the orthogonality condition. Integrating by parts twice the first integral in the left hand side of Equation (266) gives

$$\sum_{j=1}^{J+1} \rho_j \left[u_{mj}^* \frac{\partial}{\partial r}\left(\frac{\partial u_{nj}}{\partial z}\right) - \frac{\partial u_m^*}{\partial z}\ \frac{\partial u_n}{\partial r}\right]_{z_j}^{z_{j+1}} + \int_0^{z_F} \rho \frac{\partial u_n}{\partial r}\left(\frac{\partial^2}{\partial z^2} + k^2(r,z)\right) u_m^*\, dz =$$

$$-\int_0^{z_F} \rho u_m^* u_n \left(\frac{\partial k^2}{\partial r}\right) dz + k_n^2(r) \int_0^{z_F} \rho u_m^*\ \frac{\partial u_n}{\partial r}\ dz \qquad (267)$$

where no approximation has been made yet. The complex eigenfunctions and eigenvalues are used in Equation (195) to find the complex $f_n(r)$. The coupling matrices are supposed to be complex also, but under the condition of

a slowly varying range dependence the real part of the coupling integrals is very small compared to the other terms in Equation (196) and the imaginary part is even smaller because the imaginary part of the eigenfunctions and eigenvalues is much smaller than the real part. Assuming that the imaginary part of the eigenfunction is much smaller than the real part, Equation (188) may be substituted in the integral at the left hand side of Equation (267) to get the approximate expression

$$M'_{nm}(r) \simeq (M^{v}_{nm}(r) + M^{s}_{nm}(r))/(k^2_n(r) - k^2_m(r)), \qquad n \neq m \tag{268}$$

where the volume contribution is given by

$$M^{v}_{nm}(r) = \sum_{j=1}^{J+1} \rho_j \int_{z_j}^{z_{j+1}} u_{mj} u_{nj} \left[\frac{\partial k^2_j}{\partial r}\right] dz \tag{269a}$$

and the surface contribution is

$$M^{s}_{nm}(r) = \sum_{j=1}^{J+1} \rho_j \left[u_{mj} \frac{\partial}{\partial r}\left(\frac{\partial u_{nj}}{\partial z}\right) - \frac{\partial u_m}{\partial z} \frac{\partial u_n}{\partial r}\right]_{z_j}^{z_{j+1}} \tag{269b}$$

where all imaginary parts are neglected and the stratified medium of isodensity layers is used.

Since the range-independent wavenumber squared has been written in the form

$$k^2_j(z) \simeq k^2_j(z_j) + \left[\frac{k^2_j(z_{j+1}) - k^2_j(z_j)}{z_{j+1} - z_j}\right](z - z_j) \tag{270}$$

then, by linear interpolation, we obtain

$$\left.\frac{\partial k^2_j(r,z)}{\partial r}\right|_{r_i} \simeq A_{ji} z + B_{ji} \tag{271a}$$

where

$$A_{ji} = \frac{(k^2_{j+1,i} - k^2_{j,i}) - (k^2_{j+1,i-1} - k^2_{j,i-1})}{(\Delta z)_j \, (\Delta r)_i}, \tag{271b}$$

$$B_{ji} = (k^2_{j,i} - k^2_{j,i-1})/(\Delta r)_i - A_{ji} z_j, \tag{271c}$$

$$(\Delta r)_i = r_i - r_{i-1}, \tag{271d}$$

$$(\Delta z)_j = z_{j+1} - z_j, \tag{271e}$$

and

$$k^2_{n,m} = k^2_j(r_m, z_n). \tag{271f}$$

Now the volume contribution is given by,

$$M^v_{nm}(r_i) \simeq \sum_{j=1}^{J+1} \rho_j \int_{z_j}^{z_{j+1}} u_{nj}(r_i,z)\, u_{mj}(r_i,z)\, [\mathbb{A}_{ji} z + \mathbb{B}_{ji}]\, dz \tag{272}$$

or

$$M^v_{nm}(r_i) \simeq \sum_{j=1}^{J} \rho_j (\mathbb{A}_{ji}\, \mathfrak{D}_{nmji} + \mathbb{B}_{ji}\, \mathfrak{G}_{nmji}) \tag{273}$$

where $\mathfrak{D}_{nmji}$ and $\mathfrak{G}_{nmji}$ are Airy integrals of the same form as the ones in Equations (168). Since the imaginary part of the eigenfunctions have been neglected, there is no sense in using the second order perturbation term for the evaluation of these integrals. Also, the summation will go up to j=J because it has been assumed a range-independent isovelocity basement. This assumption makes $\partial k^2_{J+1}/\partial r = 0$ and it poses no restriction since we can stratify the bottom to the depth of interest, and consider from there on the so called basement layer of large thickness. With the help of Gordon's formulas we obtain $\mathfrak{D}_{nmji} = \mathfrak{I}_{nmj}$ from Equation (169d), and $\mathfrak{G}_{nmji} = \mathfrak{I}_{nmj}$ from Equation (169c) where $n \neq m$ and the subscript i only indicates the range segment into consideration.

The pressure and normal particle velocity boundary conditions are useful in reducing the surface contribution to the form

$$M^s_{nm}(r_i) = - \left[\frac{\partial u_m}{\partial z}\, \frac{\partial u_n}{\partial r}\right]_0^{z_F(r_i)} \tag{274}$$

and under the assumption of an environment that slowly varies with range this contribution is negligible compared to the volume contribution. Rutherford and Hawker[70] proved that, in an environment with range variable boundaries

and interfaces, neglicting the surface contribution results in the violation of the conservation of energy in the radial direction. However, the acoustic properties in the model in Figure 7 are the only range-dependent parameters in the problem and energy conservation is not violated.

In the case where n=m, Equation (193a) may be written as

$$M'_{nn}(r) \simeq \frac{1}{2} \sum_{j=1}^{J+1} \rho_j \int_{z_j}^{z_{j+1}} \frac{\partial}{\partial r} u_{nj}^2(r,z)\, dz \tag{275}$$

where the imaginary part of the eigenfunction has been neglected as done for the n≠m case. Since the orthonormality condition gives

$$\frac{\partial}{\partial r} \int_a^b u_n^2\, dz = \int_a^b \frac{\partial u_n^2}{\partial r}\, dz + \int_a^b u_n^2 \frac{\partial}{\partial r}\, dz = 0 \tag{276}$$

then Equation (275) becomes

$$M'_{nn}(r) \simeq -\frac{1}{2} \sum_{j=1}^{J+1} \rho_j \left[u_{nj}^2(r,z) \frac{dz(r)}{dr} \right]_{z_j}^{z_{j+1}} \tag{277}$$

which is another negligible contribution compared to the off-diagonal elements of the coupling matrix when the environment has a weak range dependence.

In conclusion, this coupling matrix is given by

$$M'_{nm}(r_i) \simeq \begin{cases} \dfrac{M^v_{nm}(r_i)}{k_n^2(r_i) - k_m^2(r_i)}, & m \neq n \\ 0, & m = n \end{cases} \tag{278}$$

where only the term with the greatest contribution has been kept. Note from Equation (269a) and (278) that $M'_{nm} = -M'_{mn}$ or that the $M'(r)$ matrix is antisymmetric. Since the eigenfunctions are considered real, then the elements of $M'(r)$ are real too. Therefore, the matrix is antihermitian and it becomes Hermitian when it is divided by i. This way it is easier and faster to diagonalize the matrix and after the diagonalization of the

Hermitian matrix, the diagonal elements must be multiplied by i to obtain the eigenvalues of $M'(r)$.

It is next to solve the coupling matrix $V(r)$ with elements given by the integral in Equation (193d). The solution is obtained with the help of the expression

$$\frac{\partial}{\partial r} u_n(r,z) = \sum_{p \neq n} M'_{np}(r)\, u_p(r,z) \tag{279}$$

which is proved by direct substitution in Equation (193a) and the use of the orthonormality condition in Equation (189). Substitution of this same expression into Equation (193d), taking the radial derivative of both terms in the summation of Equation (279), and substituting Equations (189) and (193a) gives

$$V_{nm}(r) = \frac{\partial}{\partial r} M'_{nm}(r) + \sum_{p \neq n,m} M'_{np}(r)\, M'_{pm}(r), \quad m \neq n \tag{280}$$

which is completely in terms of the previously calculated coupling matrix in Equation (278). The radial derivative of the coupling element can be simplified by acknowledging that the eigenvalues vary faster with range than the volume contribution of the coupling matrix. Then, at every range segment we obtain

$$V_{nm}(r_i) \simeq \frac{M'_{nm}(r_i)\left[\frac{dk_n^2}{dr} - \frac{dk_m^2}{dr}\right]_{r_i}}{k_m^2(r_i) - k_n^2(r_i)} + \sum_{p \neq n,m} M'_{np}(r_i)\, M'_{pm}(r_i), \quad m \neq n \tag{281}$$

where

$$\frac{dk_p^2}{dr} \simeq \frac{k_p^2(r_i) - k_p^2(r_{i-1})}{(\Delta r)_i} \tag{282}$$

always under the condition of an environment that slowly varies with range.

If n=m, the coupling term $M'_{nn}(r)$ vanishes and the radial derivative in Equation (280) is null. Since $M'(r)$ is an antihermitian matrix, Equation

(281) becomes

$$V_{nn}(r_i) \simeq - \sum_{p=1}^{N} \left[M'_{pn}(r_i)\right]^2 \qquad (283)$$

where the squared of M'(r) must be very small, but the summation of these numbers makes V(r) of considerable contribution.

The most suitable calculation of these coupling matrices has been a source of a large amount of papers. An accurate calculation of the coupling matrices takes a finely spaced sampling of the eigenfunctions and the range segments, since radial derivatives and depth integrations are required. In order to take less computer memory and time, it is appropriate to assume an environment that slowly changes with range. Another way to attack the problem is to calculate the coupling matrix in Equation (193a) directl·

The range-dependent environment is divided into range-independent segments as shown in Figure 7. The eigenvalues and eigenfunctions have been calculated for the middle of the segments at r_i and, for simplicity, the range between boundaries is the same. If the environment slowly varies with range, then Equation (193a) at the range R_i becomes

$$M'_{nm}(R_i) \simeq \int_0^{z_F} \rho(z) \left(\frac{u^*_m(r_{i+1},z)+u^*_m(r_i,z)}{2} \right) \left(\frac{u_n(r_{i+1},z)-u_n(r_i,z)}{r_{i+1}-r_i} \right) dz \qquad (284)$$

where the definition $(\Delta R)_i \equiv r_{i+1}-r_i$ and the orthonormality condition further reduces the equation to the form

$$M'_{nm}(R_i) \sim \frac{1}{2(\Delta R)_i} \sum_{j=1}^{J+1} \rho_j \int_{z_j}^{z_{j+1}} \left(u^*_{mi} u_{ni+1} - u^*_{mi+1} u_{ni} \right) dz \qquad (285)$$

where the second subscript of the complex eigenfunctions stands for the range segmentation index in the argument of the eigenfunctions in Equation (284). This equation already gives a property of the M'-matrix when the complex conjugate is taken. The property is that

$$M'_{mn} = - M'^{*}_{nm} \tag{286}$$

and only half of the off-diagonal elements have to be calculated. Setting m=n in Equation (286) also proves that the diagonal components of the matrix are purely imaginary. Since the imaginary part of the eigenvalues and eigenfunctions are much smaller than the real part, the assumption of Equation (277) being negligible is valid. Also note that this new result for $M'(r)$ is still antihermitian and can be divided by i to diagonalize the resulting Hermitian matrix.

Compare the coupling matrix as calculated in Equation (285) with the one in Equations (268) and (269). Equation (285) requires the integration over complex eigenfunctions at different range segments, while the other method only needs to be integrated over unperturbed eigenfunctions at the same range segment. The approximate solution in Equation (278) is therefore called the adiabatic approximation of $M'(r)$, since the elimination of the imaginary part of the coupling coefficients implicitly assumes that no energy in the form of heat is allowed to be transferred from one range segment to another. The integration in Equation (285) does take into account the transfer of heat from one segment to another when integrating over modes of two contiguous range segments and the imaginary part of the coupling matrix is a clear indication of the energy lost in the i^{th} segment due to this unadiabatic process. The point is to integrate Equation (285) as analytically as possible, since numerical integration is lengthy and extremely unreliable when the rapid oscillation of the higher radiating modes are taken into account.

The complex eigenfunctions in Equation (285) are the solutions of Equation (131). For Airy layers, the solution is Equation (73) where the

coefficients and the argument of the Airy functions are complex. The argument is given by Equations (85) and (84) which are now complex since the proper representation of the attenuation coefficient is by a complex sound speed. Since the sound speed may vary from range segment to another, the coefficient a in Gordon's formula, Equation (166c), is different for both functions $A[a_1(z+b_1)]$ and $B[a_2(z+b_2)]$. Therefore, another analytical formula is needed to solve Equation (285) when the eigenfunctions are a linear combination of complex Airy functions where the complex version of a_j in Equation (84c) is now given by

$$a_j = -\left(\frac{\Delta k}{\Delta z}\right)_j^{1/3} \tag{287}$$

and δ_{nj} is the same form as in Equation (84e) but complex. After calculating the complex coupling matrix M'(r), V(r) is calculated with Equations (281), (282), and (283).

If the sound speed profile does not vary much with range, an approximate formula to use is

$$\int A^*[a^*(z+b_1^*)]\, B[a\,(z+b_2)]\, dz \simeq \frac{A'^*B - A^*B'}{a^* a\,(b_1^* - b_2)} \tag{288}$$

which must be used twice to evaluate Equation (285).

Note that the adiabatic approach requires less computations and computer memory, also, in most circumstances, the oceanic acoustic properties and boundaries slowly vary with range and the adiabatic approximation seems to be the most reasonable approach. The imaginary part of the eigenvalues and eigenfunctions are not used to evaluate the coupling coefficients, but they are used to obtain the range functions in Equations (201), (206), and (222).

After the range functions are computed, the particle velocity is given by Equations (187) and (194). The transmission loss for the receiver at any depth and range larger than six wavelengths is calculated in the next section.

2.9 TRANSMISSION LOSS CALCULATION

When the signal-to-noise ratio at a sonar system is greater than a calculated *detection threshold*, it is concluded that a target is present. An accurate calculation of this detection threshold is needed for avoiding unnecessary false alarms. For passive sonar systems, where the sonar simply listens to the target, the detection threshold is given by the formula,

$$DT = SL + DI - TL - NL \tag{289}$$

where SL is the projector's source level, DI is the receiver's directivity index, TL is the media transmission loss, NL is the ambient noise level, and DT is the detection threshold for the sonar.

For an active sonar, where a sonar system or a sonobuoy listens to echoes bouncing back from the target, the calculation of the noise-limited detection threshold is given by

$$DT = SL + DI - TL_1 - TL_2 + TS - NL \tag{290}$$

where TL_1 is the transmission loss from the source to the target, TL_2 is the transmission loss from target to the receiver, and TS is called the target strength. The noise level is replaced by the reverberation level for the reverberation-limited detection threshold.

In both cases, an accurate calculation of the transmission loss is of paramount importance. The transmission loss is defined as

$$TL = -10 \log\left[\frac{I(r,z)}{I_0}\right] \tag{291}$$

where I_0 is the time-averaged reference intensity at 1 meter from the source, and the magnitude of Equation (33) provides

$$I(r,z) = | p \vec{v} | \tag{292}$$

where the pressure, p, is given by Equation (28) and the scalar potential by Equation (62). Therefore, we may decompose the time-dependent pressure field into its modal contributions,

$$p(r,z,t) = \sum_n p_n(r,z,t) \tag{293}$$

where the modal contribution for a range-independent environment is

$$p_n(r,z,t) = \frac{\omega}{4} \rho(z_0)\ \rho(z)\ u_n^*(z_0)\ u_n(z)\ H_0^{(1)}(k_n r)\ e^{i\omega t} \tag{294}$$

and direct substitution of the pressure into the transmission loss equation is known as the "coherent" loss since we are taking into account the phase factor of every mode. The transmission loss requires the time average of the intensity, and for short pulses in active sonars the ratio of energy flux density from Equation (32) must be used in Equation (291). The ratio of intensities can be used if the pulse is long enough to include the most significant multipath modes. In shallow waters, the delay between the multipath eigenrays is very small allowing a correct calculation of the transmission loss using Equation (291) with shorter pulses.

If the pulses are extremely short, then every multipath mode must be taken into account individually and the simple effects of spherical spreading and absorption are taken into account by the approximation

$$TL \simeq 20 \log(R) + \alpha R \tag{295}$$

where R is the distance travelled by the eigenray which may be calculated using the eigenray method in Reference 71 in meters, and α is the attenuation coefficient in Equation (164) where the units must be converted from kiloyards to meters. However, the constructive interference of the longer pulses yields a higher signal-to-noise ratio making them more useful in active sonar systems. For these longer pulses and for longer distances Marsh and Schulkin[72] have shown experimentally that the spreading becomes

cylindrical, the number 20 in Equation (295) becomes 10, and other correction factors dependent on the sea state and bottom properties must be added to Equation (295).

When the detailed interference effects are not of interest, they may be averaged out to yield smooth transmission loss curves. This is done by summing the individual modal energies, rather than their pressures, and the result is called "incoherent" loss. In this case, we must time-average the sum of the squares of the modal pressures. For incoherent loss, we replace Equation (291) with

$$TL = -10 \log\left[32 \left(\frac{\pi}{\omega\rho(z_0)}\right)^2 \left\langle \sum_n [\mathrm{Re}(p_n)]^2 \right\rangle \right] \tag{296}$$

where we may take the average of the sum to be the same as the sum of the average and using the asymptotic form of the Hankel function in Equation (294) we get

$$p_n(r,z,t) = \frac{\omega}{(8\pi k_n r)^{1/2}} \rho(z_0)\ \rho(z)\ u_n^*(z_0)\ u_n(z)\ e^{i(k_n r - \omega t - \pi/4)} \tag{297}$$

hence

$$\left\langle [\mathrm{Re}(p_n)]^2 \right\rangle = \frac{1}{2} |p_n|^2 = \frac{\omega^2}{16\pi k_n r} \left[\rho(z_0)\ \rho(z)\ u_n^*(z_0)\ u_n(z) \right]^2 \tag{298}$$

and the incoherent transmission loss for a range-independent environment is simply

$$TL(r,z) = -10 \log\left[\frac{2\pi\rho^2(z)}{r} \sum_n \left(\frac{u_n^2(z_0)\ u_n^2(z)}{k_n} \right) \right] \tag{299}$$

where the phases of the summed modes are immaterial when taking the magnitude squared of the eigenfunctions.

For the range-dependent environment we have calculated the velocity potential in Equation (187), therefore a transmission loss in terms of the

velocity potential most be found. The pressure is given in terms of the velocity potential in Equation (28) and the transmission loss in terms of the pressure is given by

$$TL(r,z) = -20 \log\left[\frac{p(r,z)}{p_0(0,z_0)}\right] \tag{300}$$

where p_0 is the acoustic pressure at the distance of one meter from the source and the calculation becomes incoherent when the pressure is replaced by the rms pressure. Using Equation (28), the rms pressure becomes

$$\bar{p}(r,z) = 1/\sqrt{2}\ \omega\ \rho(r,z)\ \bar{\varphi}(r,z) \tag{301}$$

and the same applies to the rms pressure at one meter from the source with the exception that the velocity potential may be given by

$$\bar{\varphi} \simeq A/(4\pi r^2) \tag{302}$$

since spherical spreading may be assumed near the source. Assuming a unitary source strength and at a distance of one meter Equation (302) becomes $\bar{\varphi}_0 \simeq 1/4\pi$ and the rms pressure at one meter is

$$\bar{p}_0 \simeq \frac{1}{\sqrt{2}}\ \frac{\omega\ \rho(0,z_0)}{4\pi} \tag{303}$$

which substituted, with Equation (301), into Equation (300) gives

$$TL(r,z) = -20 \log\left[\frac{4\pi\ \rho(r,z)}{\rho(0,z_0)}\ |\varphi(r,z)|\right] \tag{304}$$

where the complex absolute value of the velocity potential in Equation (187) must be taken. Note that the summation in Equation (299) is taken when the velocity potential is calculated.

The effects of absorption are incorporated in Equation (304) by the use of the perturbed eigenvalues, Equation (154), and eigenfunctions, Equation (161), when the attenuation coefficient $\alpha(z)$ in nepers/meter as a function of depth is given. Absorption coefficient is mostly given in dB/meter and we must convert these units. Outgoing spherical pressure waves in an isospeed

media are attenuated as

$$p(r,t) = p_0 e^{i\omega(r/c-t)-\alpha r} \tag{305}$$

and the intensity from Equation (292) is proportional to the squared of the time-averaged pressure, therefore, the absorption contribution of the transmission loss in Equation (291) becomes

$$\epsilon(r) = -20 \log(e^{-\alpha r}) \tag{306}$$

and when the reference is taken as one meter we get

$$\epsilon = [20 \log(e)]\, \alpha \tag{307}$$

or

$$\alpha \simeq 0.1151\, \epsilon \tag{308}$$

where ϵ is in dB/meter.

Another way to describe the absorption of the media is by expressing the loss in decibels per unit wavelength. This value is obtained by multiplying ϵ by the average sound speed of the media and dividing the result by the frequency of the source.

The perturbation method in Section 2.6 may also be applied to the shear wave's attenuation coefficient. The effects of shear waves from the bottom will be included in the mode coupling method in a latter report. Other approximations made are the range segmentation of the range-dependent environment as shown in Figure 7. But this should not be a great limitation since it is possible to increase the number of segments until the calculated transmission loss curves reach a state where it stays unmodified regardless of the extra segmentation. The same occurs with the depth layering of the sound velocity profile into constant speed gradients. The false resilient bottom added to the model for the discretization of the continuous spectrum can vary in depth until the transmission loss curves at the region of

interest remain steady with increasing z_F. The directivity of the source and receiver are not a problem to be added to the transmission loss calculation since they are included in the source level and directivity index of the sonar equations, respectively. Also, the frequency spectrum from a source may be modeled as a discrete number of monochromatic signals very close together and with different amplitudes. This, as well as the shear waves and three dimensional effects, remain to be included in the model.

CHAPTER 3

RESULTS

A simple environment will be considered in order to minimize the complexity of the problem and to better study the effects of range dependence of the ocean floor and the effects of its attenuation. This environment, also studied by J.Miller,[14-15] is an upslope shallow ocean similar to the one displayed in Figure 7. The water has a constant sound speed of 1500.0 m/s with a density of 1000.0 kg/m^3 and it is 200.0 meters deep from the location of the source to a range of 5.0 km. This depth decreases to 60.0 meters at a range of 10.0 km and it remains flat from there on. The bottom is one thick sediment with a resilient boundary at 1200.0 meters, a sound speed of 1704.5 m/s, a density of 1150.0 kg/m^3, and an attenuation coefficient of 8.4×10^{-4} nepers/m. Let's assume that the source is a six-blade propeller from a 112.0 meters deep submarine moving at a speed of 25 knots. Therefore, as a rule of thumb, the propeller is generating a quasi-monochromatic continuous acoustic wave with a frequency of 25.0 hertz. The range dependent environment will be divided into eight segments and the bottom's slope remains constant throughout the range dependent region of the environment.

The resulting transmission loss as a function of range and depth is given in the three-dimensional plot of Figure 8 where the range is in kilometers and the depth is in meters. A total of 18 modes have been used for this transmission loss calculation. At the position of the source, three trapped modes have been found. Note that just below the source, sound is

reflected back from the resilient false bottom regardless of the high attenuation coefficient given. However, the effects of these standing waves are negligible at the range dependent region of the environment, where the interesting phenomena occurs. Only three trapped modes exist at the range independent segment where the source is located. The source has been set to 112.0 meters deep to be located at the node of the second eigenfunction in order to excite only the first and third mode. As the bottom of the ocean decreases, the third mode gets cut-off from the water and becomes a radiating mode that propagates into the bottom sediment. This explains the low transmission loss region under the bottom of the range dependent segments of this environment. The first mode stays in the water column. Also note that there is some energy in the second mode, since the node is not exactly at 112.0 meters deep. This mode is cut-off at a range of about 9.5 kilometers from the source. The grid in this plot is divided into squares of 20.0 meters in depth and 200.0 meters in range.

If the depth of the source is set to a depth of 190.0 meters, then a second region of low transmission loss is created, as shown in Figure 9, which is caused by the convertion of the second eigenfunction to a radiating mode. Note the refracted wave created bounces back from the false bottom, but it is damped rapidly before it reaches the water column. The lower transmission loss of the refracted wave is caused by the addition of the second mode and the fact that the source is only ten meters away from the ocean floor.

If the source were located at the other side of the wedge, i.e., at 30.0 meters depth in the 60.0 meters deep semi-infinite range segment, then down-slope sound propagation occurs as shown in Figure 10. However, the

source is exciting the only mode available in this section of the ocean. As the sound propagates towards the deeper waveguide, only the fundamental mode is excited and the transmission loss plot displays no interesting feature. Since this behavior is expected, this result is a good indication that the model is performing correctly.

So far, only isovelocity layers have been used. In order to test the performance of the transmission loss calculations with layers of constant gradients in the wavenumber squared, we will include in the up-slope environment a sediment layer with z_B = 300.0 meters deep, as shown in Figure 7. This layer has a constant sound speed gradient of 0.64 s^{-1} with the sound speed at z_B equal to the one in the basement layer. Also the density and attenuation coefficient of this layer is equal to the one of the basement. The source is set back to 112.0 meters deep in order to excite the fundamental and third mode only. The resulting transmission loss surface is given in Figure 11, where only the portion over 800.0 meters deep is displayed to better observe the propagation phenomena at the sediment layer. Comparing Figure 11 to Figure 8, note that part of the energy from the third mode is propagating though the sediment and refracts back into the water column, hence the decrease in the transmission loss in the 60.0 meters deep water column. Also, due to the interaction with the sediment, some of the energy of the third mode is being used to excite the second trapped mode which becomes a radiating mode as it propagates away from the source. The second mode is not excited by the source, but by the range-dependent waveguide itself. This phenomena of energy interchange between the modes can only occur when the model allows the coupling between the modes. This is a clear indication of the high performance of this coupled normal mode model

when low frequency sound transmission loss in a range-dependent environment is needed.

CHAPTER 4

CONCLUSIONS

The coupled normal-mode model has been developed with the effects of the attenuation coefficient in all the layers of the ocean as a first and second order perturbation to the unperturbed eigenequation. It has been found that the first order perturbation term is purely imaginary and the second order perturbation term is purely real (which represents a correction to the unperturbed eigenvalue and eigenfunction). This second order perturbation term is absolutely neccesary when the attenuation coefficients are relatively high. This is the case when shear waves from the bottom sediments are included. For cases where the bottom elasticity has a very high compressional and shear attenuation coefficient, higher order perturbation terms are expected to be neccesary. In such cases, the perturbation approximation is no longer feasible and a method for searching the eigenvalues in the complex k-plane is neccesary. The theory of normal modes with the effects of the bottom's elastic properties and a method of searching for the complex eigenvalues is underway and will be presented in future publications. Also, the effects of three-dimensional sound propagation using an extended version of the coupled normal-mode model will be modeled.

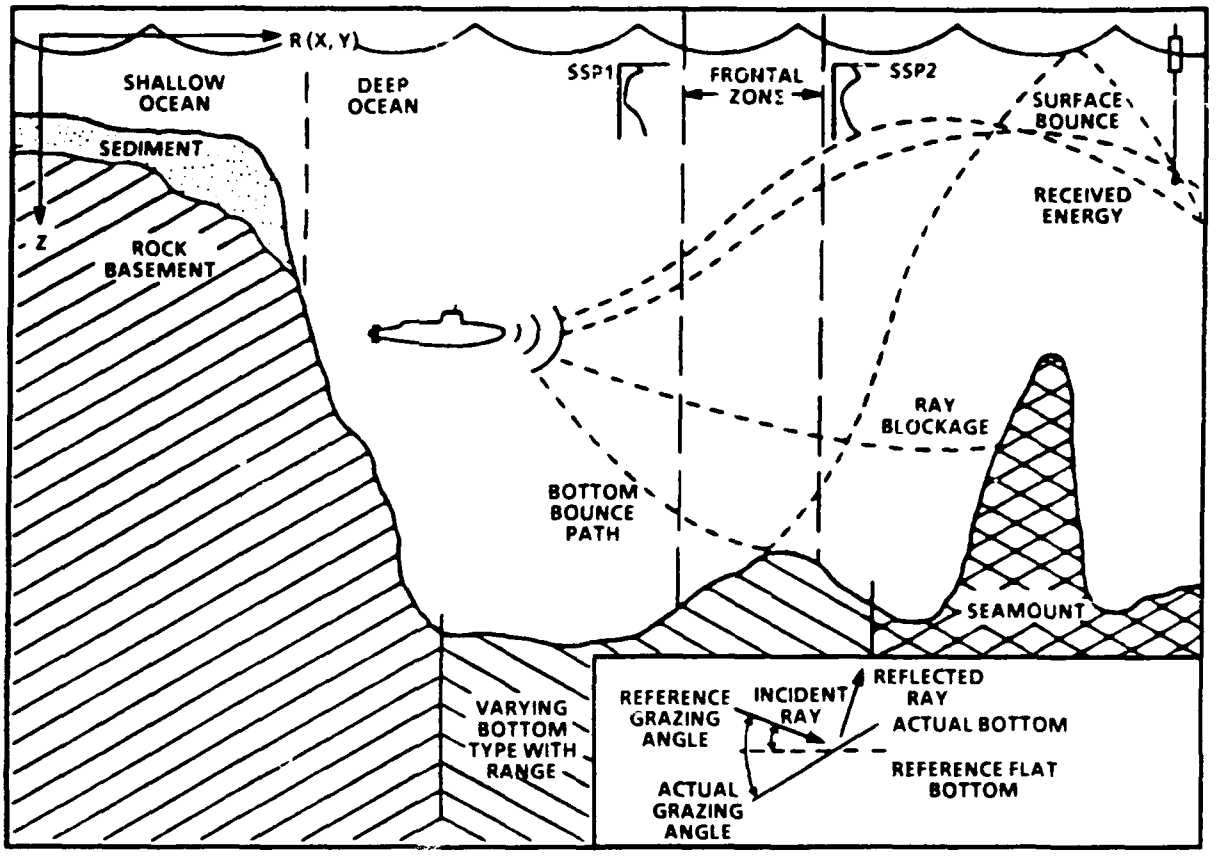

FIGURE 1. ACOUSTIC RAY THEORY IN THE DEEP OCEAN (ACOUSTIC NORMAL MODES MUST BE USED IN THE SHALLOW OCEAN)

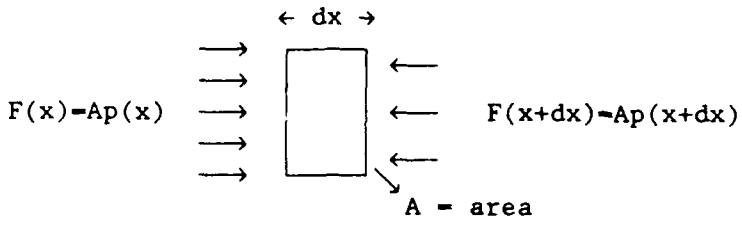

(a) FOR THE EULER EQUATION OF MOTION

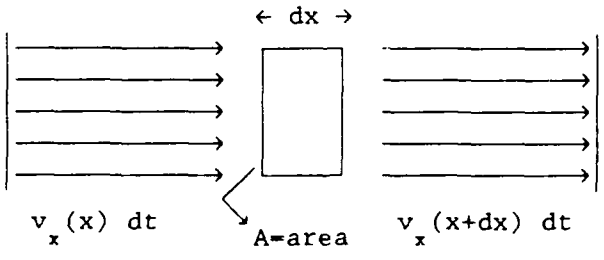

(b) FOR THE CONTINUITY EQUATION

FIGURE 2. DEVRIVATION MODELS

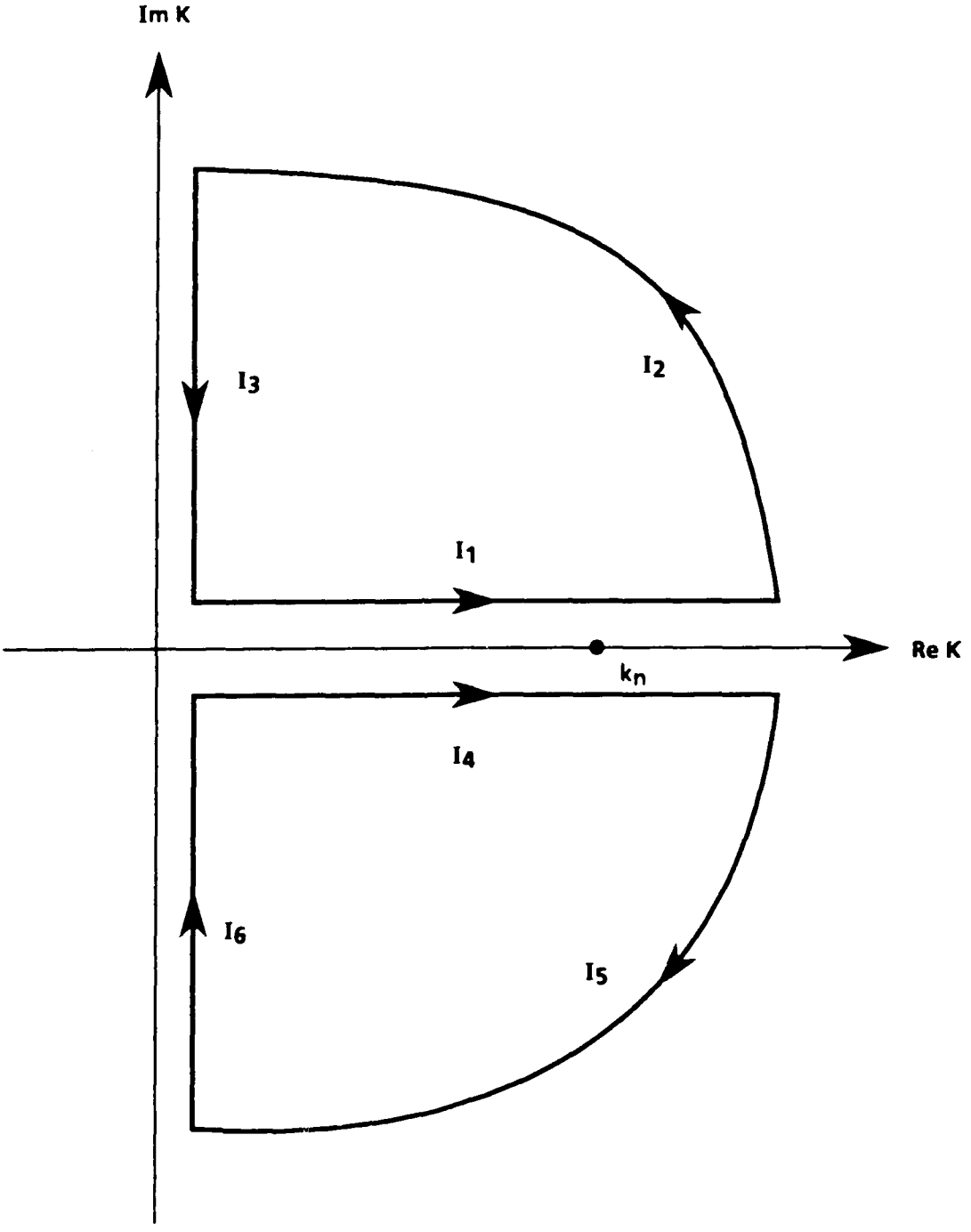

FIGURE 3. PATHS OF INTEGRATION USED FOR THE EVALUATION OF THE CONTRIBUTION OF THE POLES

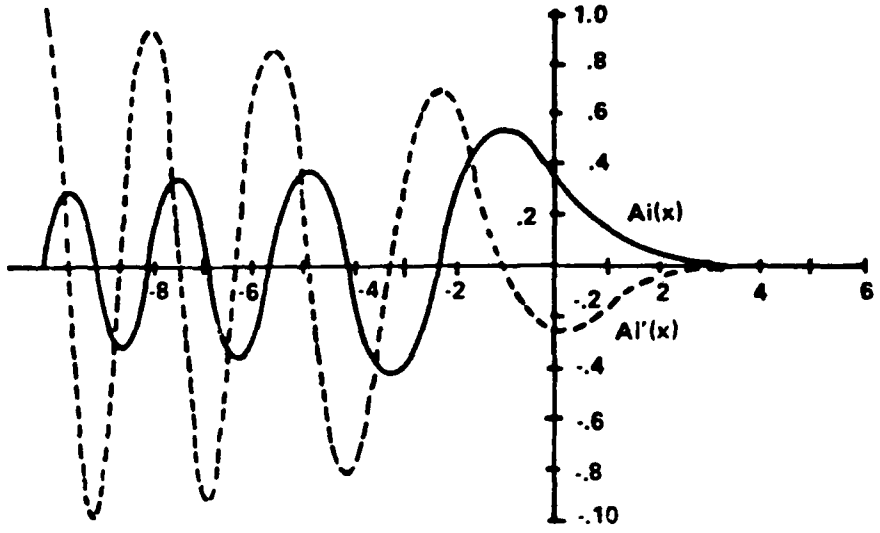

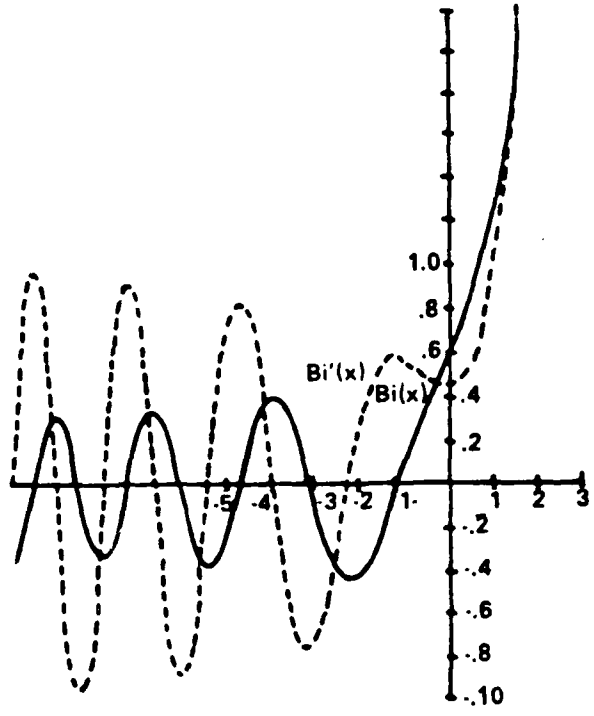

FIGURE 4. THE AIRY FUNCTIONS AND THEIR FIRST DERIVATIVE

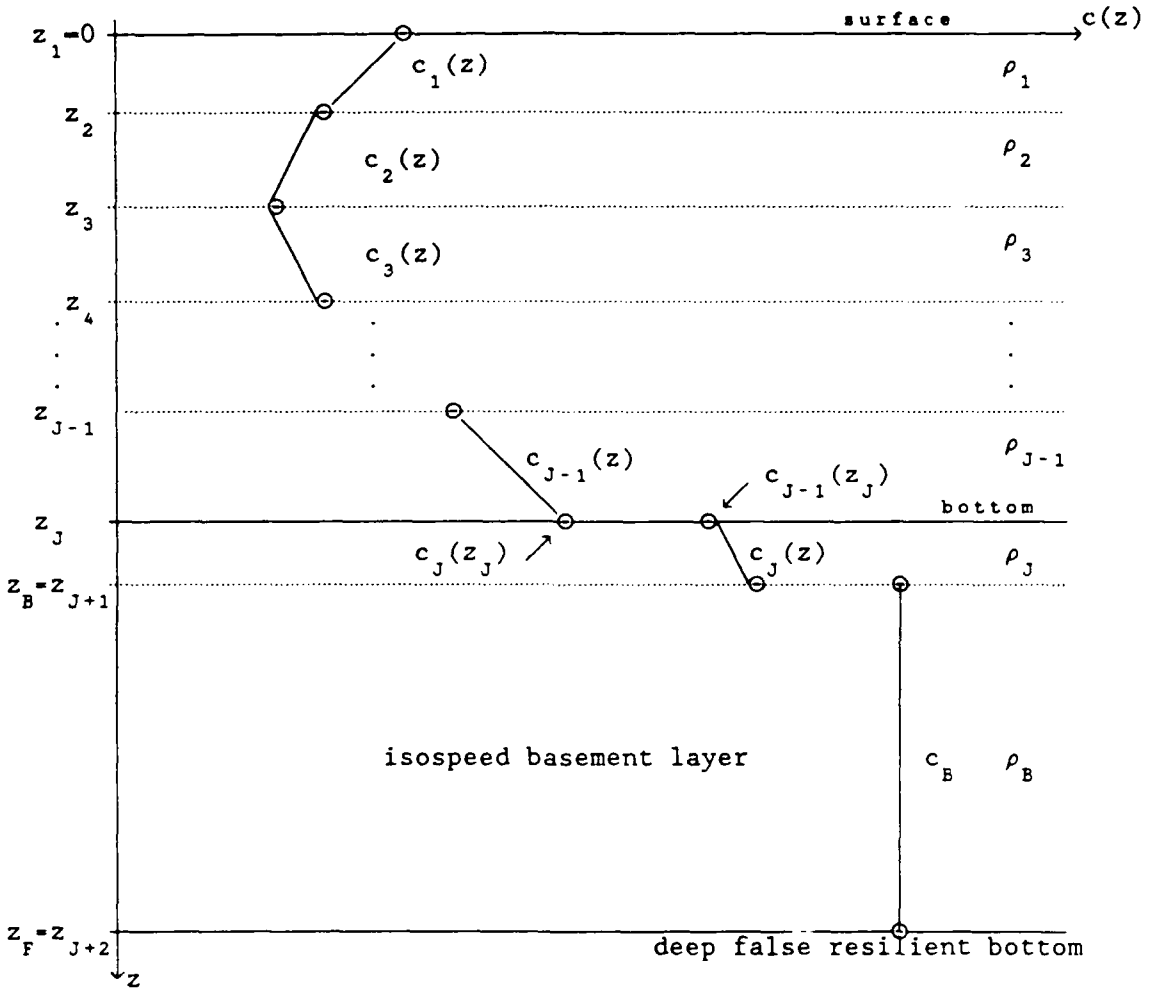

FIGURE 5 THE GENERAL STRATIFIED RANGE-INDEPENDENT OCEAN ENVIRONMENT MODEL

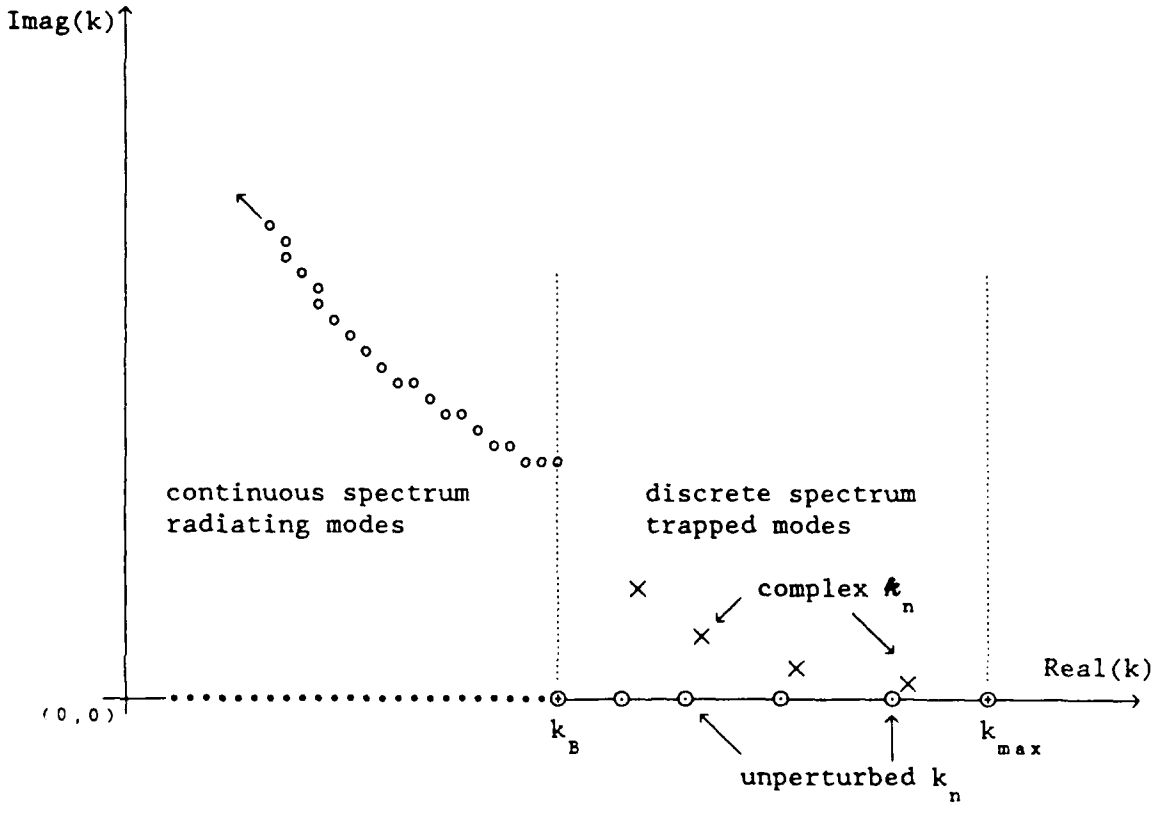

FIGURE 6. EXPECTED MIGRATION OF EIGENVALUES WHEN COMPRESSIONAL ABSORPTION IS INTRODUCED

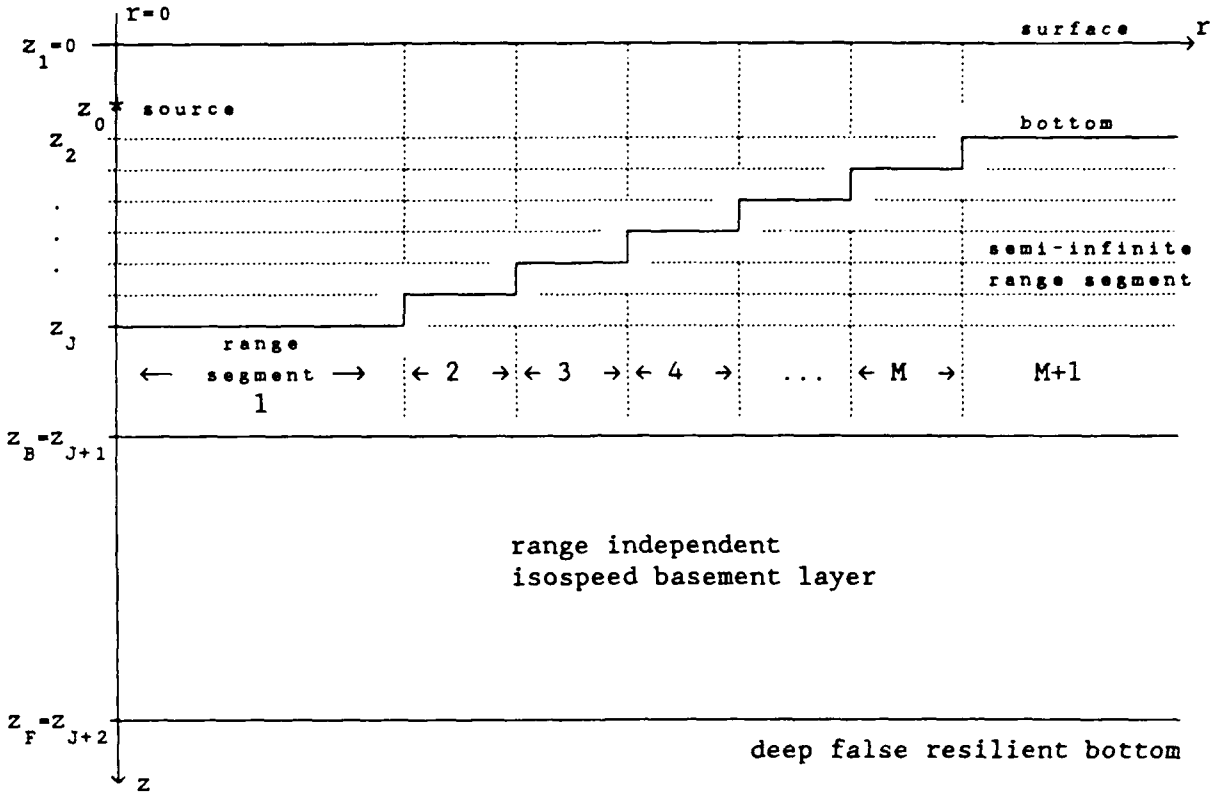

FIGURE 7. THE RANGE-DEPENDENT ENVIRONMENT DIVIDED INTO M + 1 RANGE-INDEPENDENT SEGMENTS WHERE THE SOURCE IS AT THE FIRST SEGMENT AND A VERY DEEP RESILIENT BOTTOM IS INCLUDED TO DISCRETIZE THE CONTINUOUS SPECTRUM

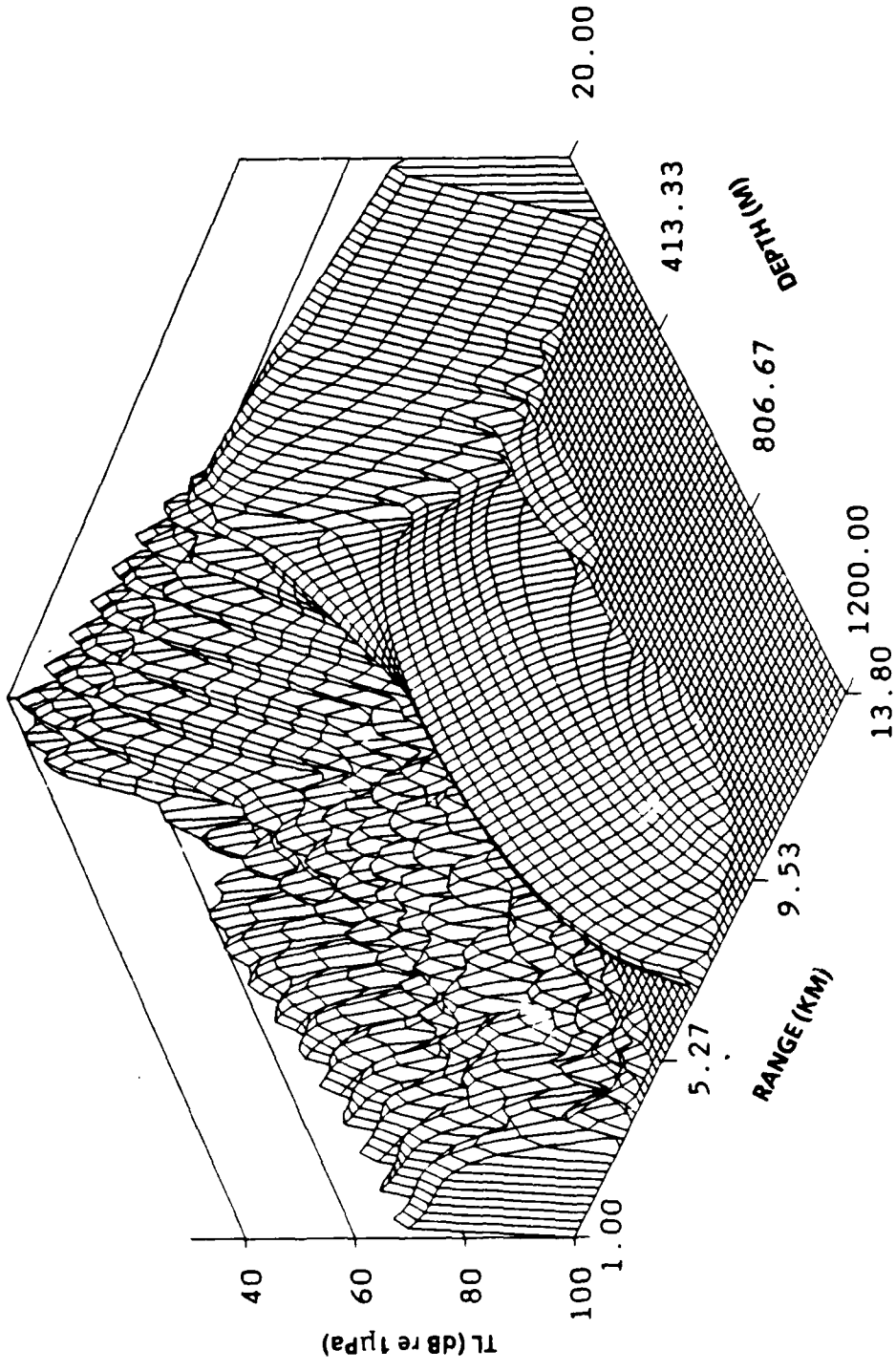

FIGURE 8. UP-SLOPE TRANSMISSION LOSS (EIGHTEEN MODES WERE COUPLED; SOURCE DEPTH IS 112.0 METERS)

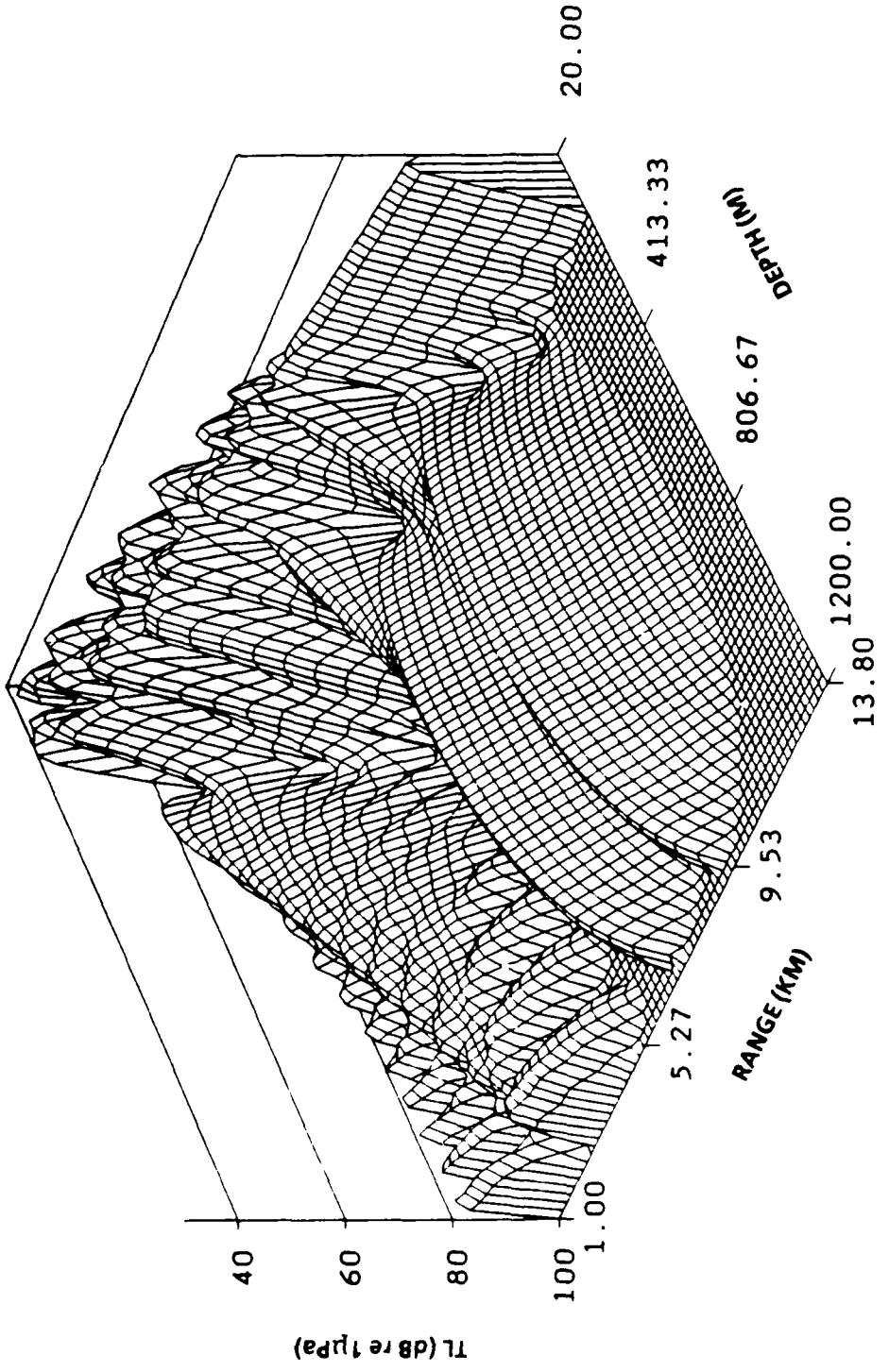

FIGURE 9. UP-SLOP TRANSMISSION LOSS (SOURCE DEPTH IS 190.0 METERS TO EXCITE THE SECOND MODE)

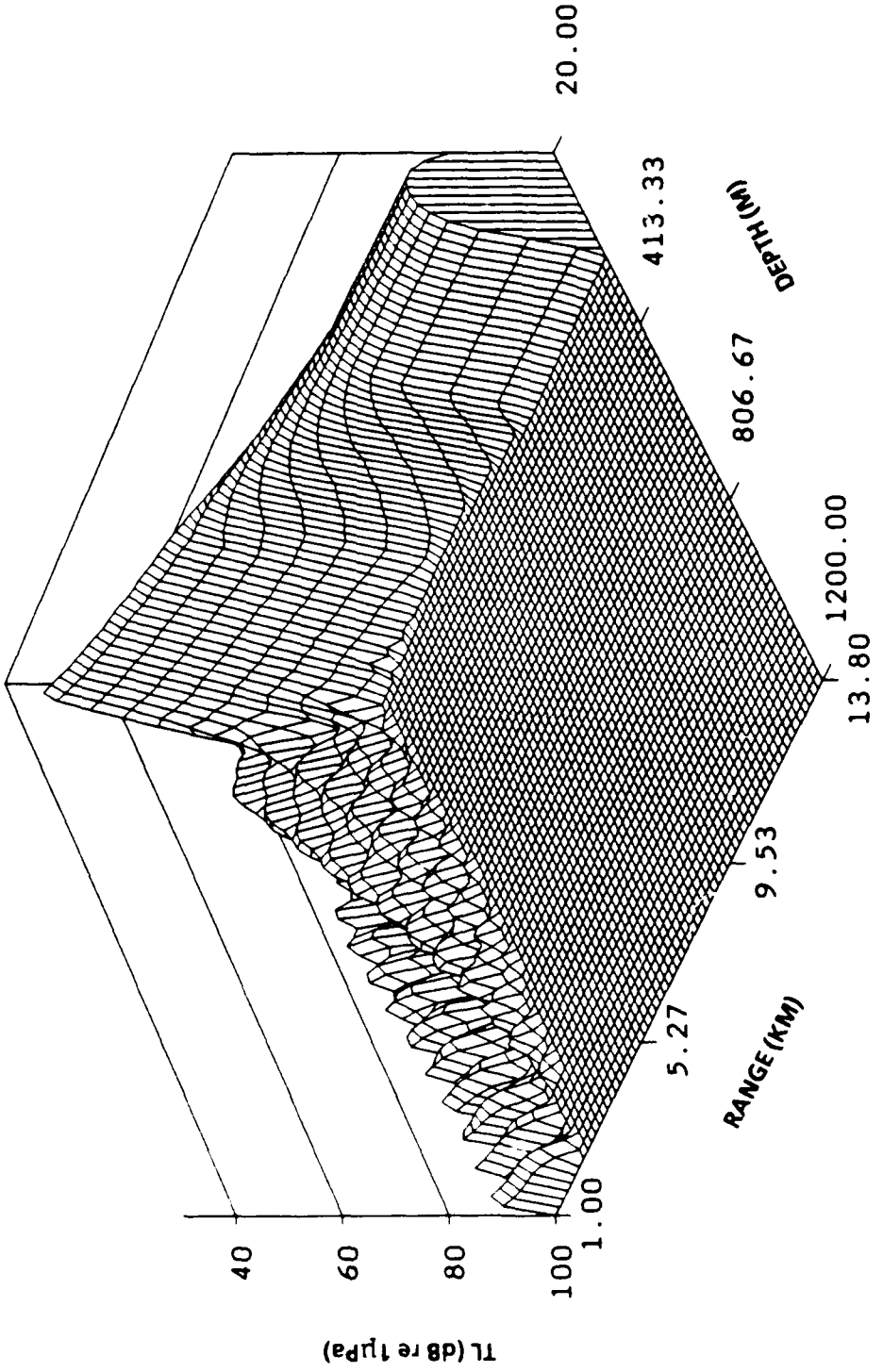

FIGURE 10. DOWN-SLOPE TRANSMISSION LOSS (SOURCE DEPTH IS 30.0 METERS AND ONLY THE FUNDAMENTAL MODE CAN BE EXCITED)

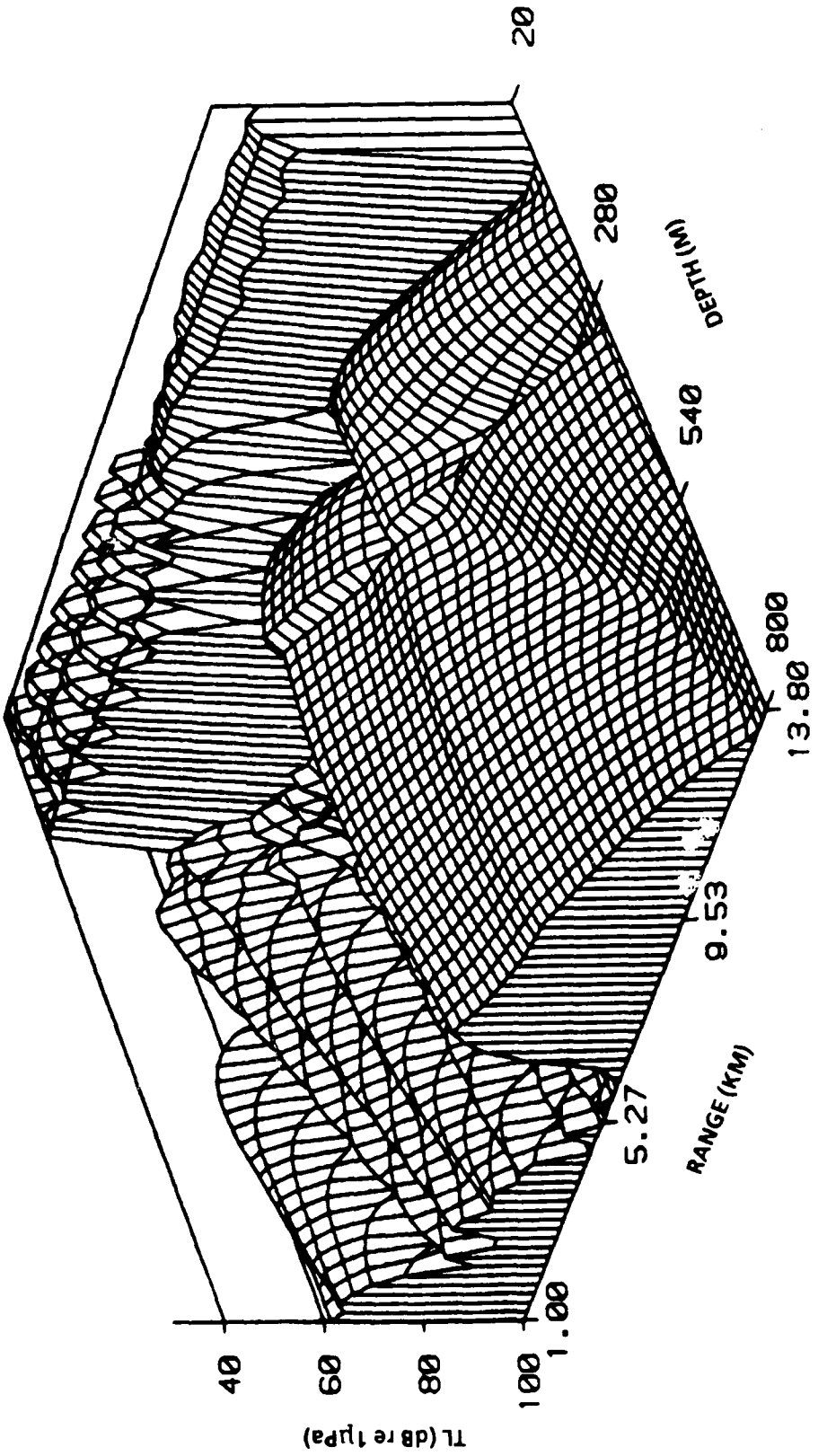

FIGURE 11. UP-SLOPE TRANSMISSION LOSS (SOURCE DEPTH IS 112.0 METERS; A BOTTOM SEDIMENT WITH POSITIVE SOUND SPEED GRADIENT IS INCLUDED)

REFERENCES

1. Pierce, A., "Extension of the Method of Normal Modes to Sound Propagation in an Almost-Stratified Medium," Acoustical Society of America Journal, Vol. 37, No. 1, 1965, p. 19.

2. Pierce, A., "Parametric Solution of the Dispersion Relation for Guided Sound Propagation in Shallow Water," Acoustical Society of America Journal, Vol. 39, No. 6, 1966, p. 1139.

3. Pierce, A., "Guided Mode Disappearance during Upslope Propagation in Variable Depth Shallow Water Overlying a Fluid Bottom," Acoustical Society of America Journal, Vol. 72, No. 2, 1982, p. 523.

4. Pierce, A., "Augmented Adiabatic Mode Theory for Upslope Propagation from a Point Source in Variable-Depth Shallow Water Overlying a Fluid Bottom," Acoustical Society of America Journal, Vol. 74, No. 6, 1983, p. 1837.

5. McDaniel, S., "Coupled Power Equations for Cylindrically Spreading Waves," Acoustical Society of America Journal, Vol. 60, No. 6, 1976, p. 1285.

6. McDaniel, S., "Mode Conversion in Shallow-Water Sound Propagation," Acoustical Society of America Journal, Vol. 62, No. 5, 1977, p. 320.

7. McDaniel, S., "Calculation of Mode Conversion Rates," Acoustical Society of America Journal, Vol. 63, No. 5, 1978, p. 1372.

8. McDaniel, S. and McCammon, D., "Mode Coupling and the Environmental Sensitivity of Shallow-Water Propagation Loss Predictions," Acoustical Society of America Journal, Vol. 82, No. 1, 1987, p. 217.

REFERENCES (Cont.)

9. Evans, R., "A Coupled Mode Solution for Acoustic Propagation in a Waveguide with Stepwise Depth Variations of a Penetrable Bottom," Acoustical Society of America Journal, Vol. 74, No. 1, 1983, p. 188.

10. Evans, R. and Gilbert, K., "The Periodic Extension of Stepwise Coupled Modes," Acoustical Society of America Journal, Vol. 77, No. 3, 1985, p. 983.

11. Evans, R., "The Decoupling of Stepwise Coupled Modes," Acoustical Society of America Journal, Vol. 80, No. 5, 1986, p. 1414.

12. Graves, R., Nagl, A., Überall, H., and Zarur, G., "Range-Dependent Normal Modes in Underwater Sound Propagation: Application to the Wedge-Shaped Ocean," Acoustical Society of America Journal, Vol. 58, No. 6, 1975, p. 1171.

13. Nagl, A., Überall, H., Haug, A., and Zarur, G., "Adiabatic Mode Theory of Underwater Sound Propagation in a Range-Dependent Environment," Acoustical Society of America Journal, Vol. 63, No. 3, 1978, p. 739.

14. Miller, J., Range-Dependent Normal-Mode Calculations of Acoustic Propagation in the Ocean Including Effects of Layered-Bottom Penetration, Ph.D. Dissertation, Catholic University of America, Washington D.C., 1985.

15. Miller, J., Nagl, A., and Überall, H., "Upslope Sound Propagation through the Bottom of a Wedge-Shaped Ocean beyond Cutoff," Acoustical Society of America Journal, Vol. 79, 1986, p. 562.

16. Ali, H., Arvelo, J., Nagl, A., and Überall, H., "Sound Interaction with a Sloping, Upward-refracting Ocean Bottom," Acoustical Society of America Journal, Vol. 82, No. S61, 1987.

REFERENCES (Cont.)

17. Miller, J., Collins, M., Ali, H., Arvelo, J., Nagl, A., and Überall, H., "Sound Penetration into a Sloping Ocean Floor," II FASE Conference, Madrid, Spain, 19 Jun 1987.

18. Collins, M., Ali, H., Authement, M., Nagl, A., Überall, H., Miller, J., and Arvelo, J., "Low-Frequency Sound Interaction with a Sloping, Refracting Ocean Bottom," IEEE Journal of Ocean Engineering, Vol. 13, No. 4, Oct 1988, p. 235.

19. Arvelo, J., Talmant, M., Bazow, T., Miller, J., Nagl, A., and Überall, H., "Ocean Bottom Absorption and Shear Effects and 3D Effects in Coupled Mode Propagation Theory," 3D Acoustics working group workshop, University of Southern Mississippi, Long Beach, MS, 7 Jul 1988.

20. Arvelo, J., Talmant, M., and Überall. H., "A Coupled-Mode Method for Sound Interaction with an Elastic Oceanic Bottom," Acoustical Society of America Journal, Vol. 84, No. S91, Fall 1988.

21. Thompson. W., "Transmission of Elastic Waves through a Stratified Solid Medium," Applied Physics Journal, Vol. 21, 1950, p. 89.

22. Kornhauser, E. and Raney, W., "Attenuation in Shallow-Water Propagation due to an Absorbing Bottom," Acoustical Society of America Journal, Vol. 27, No. 4, 1955, p. 689.

23. Williams, A. and Eby, R., "Acoustic Attenuation in a Liquid Layer Over a 'Slow' Viscoelastic Solid," Acoustical Society of America Journal, Vol. 34, No. 6, 1962, p. 836.

24. Bucker, H., "Sound Propagation in a Channel with Lossy Boundaries," Acoustical Society of America Journal, Vol. 48, No. 5, 1970, p. 1187.

25. Folds, D. and Loggins, C., "Transmission and Reflection of Ultrasonic Waves in Layered Media," Acoustical Society of America Journal, Vol. 62, No. 5, 1977, p. 1102.

REFERENCES (Cont.)

26. Ingenito, F., Ferris, R., Kuperman, W., and Wolf, S., Shallow Water Acoustics, NRL Report 8179, 27 Mar 1978, Naval Research Laboratory, Washington, DC.

27. Mitchell, S. and Focke, K., "The Role of the Sea Bottom Attenuation Profile in Shallow Water Acoustic Propagation," Acoustical Society of America Journal, Vol. 73, No. 2, 1983, p. 465.

28. Koch, R., Vidmar, P., and Lindberg, J., "Normal Mode Identification for Impedance Boundary Conditions," Acoustical Society of America Journal, Vol. 73, No. 5, 1983, p. 1567.

29. Chapman, N., "Modeling Ocean-Bottom Reflection Loss Measurements with the Plane-wave Reflection Coefficient," Acoustical Society of America Journal, Vol. 73, No. 5, 1983, p. 1601.

30. Porter, M. and Reiss, E., "A Numerical Method for Ocean-Acoustic Normal Modes," Acoustical Society of America Journal, Vol. 76, No. 1, 1984, p. 244.

31. Hooshyar, M., "An Inverse Scattering Problem of Elastic Waves," Acoustical Society of America Journal, Vol. 77, No. 3, 1985, p. 844.

32. Porter, M. and Reiss, E., "A Numerical Method for Bottom Interacting Ocean Acoustic Normal Modes," Acoustical Society of America Journal, Vol. 77, No. 5, 1985, p. 1760.

33. Ellis, D. and Chapman, D., "A Simple Shallow Water Propagation Model Including Shear Wave Effects," Acoustical Society of America Journal, Vol. 78, No. 6, 1985, p. 2087.

34. Beebe, J. and Holland, C., "Shallow-Water Propagation Effects over a Complex, High-Velocity Bottom," Acoustical Society of America Journal, Vol. 80, No. 1, 1986, p. 244.

REFERENCES (Cont.)

35. Jackins, P., Gaunaurd, G., and Arvelo, J., "Resonance Reflections from a Stratified Ocean Bottom," Acoustical Society of America Journal, Vol. 80, No. S116, 1986.

36. Koch, R. and Vidmar, P., "Shear Wave Effects on Propagation to Near-Bottom and Sub-Bottom Receivers," Acoustical Society of America Journal, Vol. 81, No. 2, 1987, p. 269.

37. Zhou, J. and Zhang, X., "Effect of Frequency Dependence of Sea-Bottom Attenuation on the Optimum Frequency for Acoustic Propagation in Shallow Water," Acoustical Society of America Journal, Vol. 82, No. 1, 1987, p. 287.

38. McDonal, F., Angona, F., Mills, R., Sengbush, R., Van Nostrand, R., and White, J., "Attenuation of Shear and Compressional Waves in Pierre Shale," Geophysics, Vol. 23, No. 3, 1958, p. 421.

39. McCann, C. and McCann, M., "The Attenuation of Compressional Waves in Marine Sediments," Geophysics, Vol. 34, No. 6, 1969, p. 882.

40. Stroll, R. and Bryan, G., "Wave Attenuation in Saturated Sediments," Acoustical Society of America Journal, Vol. 47, No. 5, 1970, p. 1440.

41. Hamilton, E., "Sound Attenuation as a Function of Depth in the Sea Floor," Acoustical Society of America Journal, Vol. 59, No. 3, 1976, p. 528.

42. Hamilton, E., "Attenuation of Shear Waves in Marine Sediments," Acoustical Society of America Journal, Vol. 60, No. 2, 1976, p. 334.

43. Francis, T., "The Ratio of Compressional to Shear Velocity and Rock Porosity on the Axis of the Mid-Atlantic Ridge," Geophysical Resesearch Journal, Vol. 81, No. 23, 1976, p. 4361.

REFERENCES (Cont.)

44. Hamilton, E., "Shear-Wave Velocity versus Depth in Marine Sediments: A Review," Geophysics, Vol. 41, No. 5, 1976, p. 985.

45. Shirley, D. and Hampton, L., "Shear-Wave Measurements in Laboratory Sediments," Acoustical Society of America Journal, Vol. 63, No. 2, 1978, p. 607.

46. Hamilton, E., "Sound Velocity Gradients in Marine Sediments," Acoustical Society of America Journal, Vol. 65, No. 4, 1979, p. 909.

47. Hamilton, E., "Geoacoustic Modeling of the Sea Floor," Acoustical Society of America Journal, Vol. 68, No. 5, 1980, p. 1313.

48. Brunson, B. and Johnson, R., "Laboratory Measurements of Shear Wave Attenuation in Saturated Sand," Acoustical Society of America Journal, Vol. 68, No. 5, 1980, p. 1371.

49. Werby, M. and Tango, G., "Characterization of Average Geoacoustic Bottom Properties from Expected Propagation Behavior at Very Low Frequencies using a Towed Array Simulation," Ocean Seismo-Acoustics, Jun 1985, p. 881.

50. Hamilton, E., "Sound Velocity as a Function of Depth in Marine Sediments," Acoustical Society of America Journal, Vol. 78, No. 4, 1985, p. 1348.

51. Carey, W., "Measurement of Down-Slope Sound Propagation from a Shallow Source to a Deep Ocean Receiver," Acoustical Society of America Journal, Vol. 79, No. 1, 1986, p. 49.

52. Matsumoto, E. and Nagaoka, H., "Stress Measurement Using Vertically Polarized Shear Waves," Wave Motion, Vol. 8, 1986, p. 571.

REFERENCES (Cont.)

53. Stoll, R., Flood, B., Flood, R., Chayes, D., and Manley, P., "Shallow Seismic Experiments Using Shear Waves," Acoustical Society of America Journal, Vol. 83, No. 1, 1988, p. 93.

54. Kuperman, W. and Jensen, F., Bottom-Interacting Ocean Acoustics, Plenum Press, New York, NY, 1980.

55. Etter, P. and Flum, R., "A Survey of Underwater Acoustic Models and Environmental-Acoustic Data Bases," ASWR-80-115, Sep 1980, ASW Systems Project Office.

56. Etter, P., "Numerical Modeling Techniques in Underwater Acoustics," Acoustical Society of America Journal, Vol. 82, No. S102, 1987.

57. Schulten, Z., Anderson, D., and Gordon, R., "An Algorithm for the Evaluation of the Complex Airy Functions," Computational Physics Journal, Vol. 31, 1979, p. 60.

58. Boyles, A., Acoustic Waveguides, Applications to Oceanic Science, John Wiley & Sons, New York, NY, 1984, Chapter 4.

59. Love, A., A Treatise on the Mathematical Theory of Elasticity, Dover, Toronto, Ontario, 1944.

60. Ewing, W., Jardetzky, W., and Press, F., Elastic Waves in Layered Media, McGraw-Hill, New York, NY, 1957.

61. Auld, B., Acoustic Fields and Waves in Solids, John Wiley & Sons, New York, NY, 1973.

62. Aki, K. and Richards, P., Quantitative Seismology: Theory and Methods, Freeman and Company, New York, NY, 1980.

63. Skudrzyk, E., The Foundations of Acoustics, Springer-Verlag, New York, NY, 1971.

REFERENCES (Cont.)

64. Brekhovskikh, L., Waves in Layered Media, Academic Press, New York, NY, 1980.

65. Urick, R., Principles of Underwater Sound for Engineers, McGraw-Hill, New York, NY, 1975.

66. Dennis, J. and Schnabel, R., Numerical Methods for Unconstrained Optimization and Nonlinear Equations, Prentice-Hall, Englewood Cliffs, NJ, 1983.

67. Gordon, R., "New Method for Constructing Wavefunctions for Bound States and Scattering," Chemical Physics Journal, Vol. 51, 1969, p. 14.

68. Gordon, R., "Quantum Scattering Using Piecewise Analytic Solutions," Methods in Computational Physics, Vol. 10, Academic Press, 1971.

69. Anderson, E., Modern Physics and Quantum Mechanics, W.B.Saunders, New York, NY, 1971.

70. Rutherford, S. and Hawker, K., "Consistent Coupled Mode Theory of Sound Propagation for a Class of Nonseparable Problems," Acoustical Society of America Journal, Vol. 70, No. 2, 1981, p. 554.

71. Arvelo, J., Eigenray Calculations in a Uniformly Stratified Multilayered Medium, NSWC TR 86-258, 27 Jun 1986, NSWC, White Oak, MD.

72. March, H. and Schulkin, M., "Shallow Water Transmission," Acoustical Society of America Journal, Vol. 31, 1962, p. 863.

DISTRIBUTION

	Copies
Office of Naval Research Code 1122 800 N. Quincy St., BCT#1 Arlington, VA 22217	1
Naval Underwater Systems Center Attn: Library New London, CT 06320	1
Naval Underwater Systems Center Attn: Library Newport, RI 02841-5047	1
Naval Ocean Systems Center Attn: Library San Diego, CA 92152	1
Naval Air Development Center Attn: Library Warminster, PA 18974	1
Naval Coastal Systems Center Attn: Library Panama City, FL 32401	1
Naval Research Laboratory Attn: Library Washington, DC 20390	1
Naval Sea Systems Command Attn: Library Washington, DC 20362	1
Superintendent Naval Postgraduate School Attn: Library Monterrey, CA 93940	1

	Copies
Defense Advanced Research Project Agency 1400 Wilson Blvd. Arlington, VA 22209	1
Defence Technical Information Center Cameron Station Alexandria, VA 22314	2
Internal Distribution:	
E231	2
E232	15
E342 (GIDEP)	1
R04 (C. Dickinson)	1
U (B. Gay)	1
U02 (J. Goeller)	1
U04 (M. Stripling)	1
U20 (C. Kalivretenos)	1
U202 (T. Ballard)	1
U25 (J. Sherman)	1
U25 (D. Watts)	1
U25 (J. Arvelo)	10
U25 (S. Hebbert)	1